Approaching finite density QCD using Complex Langevin Simulation

I.-O. Stamatescu (Heidelberg)

Results in the frame of common work with:

G. Aarts (Swansea), E. Seiler (Munich) and D. Sexty (Heidelberg)

and further collaboration with

L. Bongiovanni and J. Pawlowski (Heidelberg).

Workshop on *Finite Density QCD* KEK 2014

Items of the discussion

1. Some introduction and motivation
2. CLE: set up, proofs and problems
3. Tests in effective models
4. Controlling the method for gauge models: Gauge Cooling
5. Analysis of a realistic gauge model: HDQCD
6. Results for full QCD
7. Discussion
8. Appendix (bibliography, technicalities, additional figures)

1. Introduction

What is CLE and what is it good for?

- Euclidean LGT:
  QFT path integral $\longrightarrow$ partition function $\longrightarrow$ simulation (importance sampling)
- Averages with the partition function $\longrightarrow$ averages over a stochastic process in a discretized "5-th" time (the CPU time ...):
  1. Monte Carlo (MC) simulations (Metropolis, Heat Bath, etc: only statistical errors: no discretization dependence).
     Needs a probability interpretation of the Boltzmann factor $\leftrightarrow$ real action
  2. Random Walk (RW) or Langevin Equation (LE) (discretization errors, can be eliminated)
     Does not need a probability interpretation of the Boltzmann factor (in fact, not even an action!)

(Real) Langevin Equation and Random Walk.

Here in discretized form, Ito calculus, ϑ: 5-th "time", $\delta\vartheta$: "time" step; for a field $\varphi(x)$ (random variable), $K[\varphi]$: drift force,

Langevin equation:

$$\begin{aligned}\delta\varphi(x;\vartheta) \;\equiv\; & \varphi(x;\vartheta+\delta\vartheta)-\varphi(x;\vartheta) = K[\varphi(x;\vartheta)]\,\delta\vartheta + \eta(x;\vartheta) \\ & \langle\eta(x;\vartheta)\rangle = 0, \quad \langle\eta(x;\vartheta)\eta(x';\vartheta')\rangle = 2\,\delta\vartheta\,\delta_{x,x'}\,\delta_{\vartheta,\vartheta'}\end{aligned}$$

Random Walk:

$$\delta\varphi(x;\vartheta) = \pm\omega, \quad \text{with pbb}: \;\; \tfrac{1}{2}(1 \pm \tfrac{1}{2}\omega\, K[\varphi(x;\vartheta)])\,, \;\; \omega = \sqrt{\delta\vartheta}$$

In the following we shall use t insead of ϑ.

Relation to path integral

If the drift is the gradient of a real action, bounded from below **then** there is a probability density $P(\varphi, t)$ satisfying an associated Fokker-Planck Equation (FPE) in the limit $\delta t \longrightarrow 0$:

$$\partial_t P(\varphi, t) = \partial_\varphi \left(\partial_\varphi - K\right) P(\varphi, t), \quad K = -\partial_\varphi S$$

and we have:

$$P(\varphi, t) = c_0 \mathrm{e}^{-S[\varphi]} + \sum_{E_n > 0} c_n \phi_n \mathrm{e}^{-E_n t} \to P_{as}(\varphi) = c_0 \mathrm{e}^{-S[\varphi]}, \ (t \to \infty)$$

with E_n the *eigenvalues* of the Fokker–Planck Hamiltonian:

$$\mathrm{H_{FP}} = -\partial_\varphi^2 + \frac{1}{4}(\partial_\varphi S)^2 - \frac{1}{2}(\partial_\varphi^2 S)$$

Thus:

- The stationary distribution of the variables reproduces the original Boltzman factor.
- The convergence is controlled by the properties of the FP Hamiltonian,
- Expectation values $\langle f(\varphi)\rangle$ can be calculated as averages over the noise, equivalently as t averages:

$$\overline{f(\varphi)} = \frac{1}{T}\int_0^T dt\, f(\varphi(t)) = \langle f(\varphi)\rangle + \mathcal{O}(1/\sqrt{T})\,,$$

- In practice $\delta t \neq 0$: $\rho_{as}(\varphi)$ has $\mathcal{O}(\delta t)$ corrections (controllable).

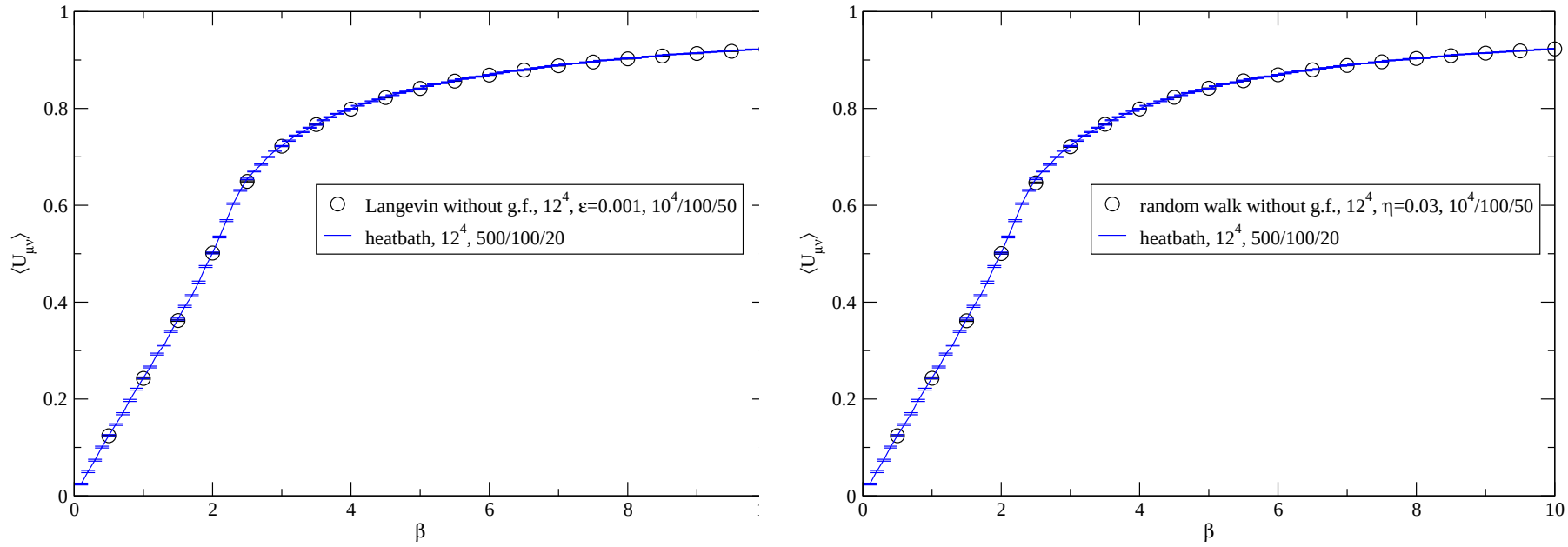

Figure 1: Plaquette averages by LE and RW compared with MC

For a general discussion and application to Gauge Theory see
G. Batrouni, G. Katz, A. Kronfeld, G. Lepage, B. Svetitsky, K. Wilson, PRD 1985

CLE is the extension of the LE algorithm to the case of complex action.

This is possible *in principle* since the process does not rely on a probability interpretation of the Boltzman factor.

What shall we do with the complex action?

What shall we do with the drunken sailor? (3 times)

... early in the morning ..

Hey, ho and up she rises (3 times)

Put'im in the longboat till he's over ... (3 times)

Put him in the bed of the captain daughter ... (3 times)

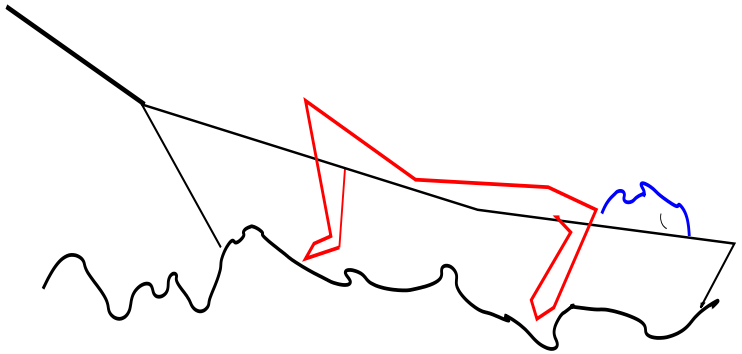

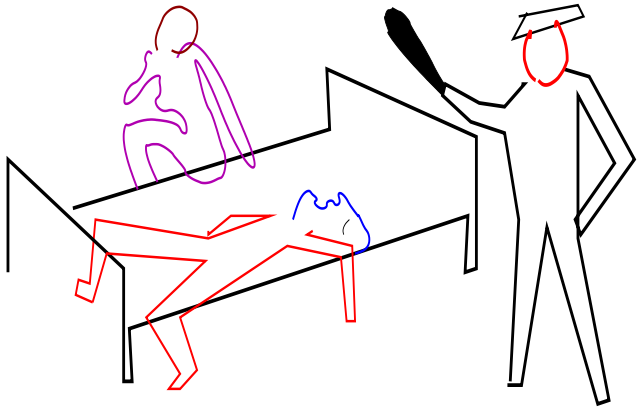

Not known, which solution was better ...

Typical Problems with complex action:

1. real time simulations, non-equilibrium QFT
   J. Berges and IOS, PRL 2005; J. Berges, S. Borsanyi, D. Sexty, IOS, PRD 2007; J. Berges, D. Sexty, NPhB 2008
2. *chemical potential*
3. $\theta-$ term ... *L. Bongiovanni et al, Lattice 2013*

CLE provides in all these cases an approach - sometimes, the only one $\longrightarrow$ develop this approach to a reliable method.

Here we discuss the problems, the possibilities to control them, and show applications.

Much work since the original papers of *Parisi* and of *Klauder (1983)*, both theoretical and aplicative, here only a few:

H. Hueffel, H. Rumpf, PLB 1984; F. Karsch, H. Wyld, PRL 1985; H. Gausterer, J. Klauder, PRD 1986; T. Matsui, A. Nakamura, 1986; J. Ambjorn, M. Flensburg, C. Peterson, NPhB 1986; J. Flower, S. Otto, S. Callahan, PRD 1986; M. Fukugita, Y. Oyanagi, A. Ukawa, PRD 1987; K. Okano, L. Schulke, B. Zheng PLB 1991; K. Fujimura, K. Okano, L. Schulke, K. Yamagishi, B. Zheng, NPhB 1994; ...

Interest went down when difficulties appeared.

New interest in connection with problems for which no other general solution is available: non-eqilibrium QFT, QCD at non-zero density, ...

The present general work and our working programme :

1. Theoretical discussion [A, 3].
2. Study the various aspects of the problem on simple, soluble models used as effective models, Random matrices, Thirring model [A, 1, 2, 4].
3. Extend the analysis to more complex models with non-trivial phase structure XY-model, $SU(3)$ spin model [A].
4. Extend the analysis to full QCD-approximations (HDQCD) [A, 5].
5. Study full QCD [A].

Our group [A] and *beyond:* *C. Pehlevan, G. Guralnik, NPhB 2009* [1]; *J. Pawlowski, C. Zielinski, PRD 2013* [2]; *A. Duncan, M. Niedermaier, Ann.Ph. 2013* [3]; *A. Mollgaard, K. Splittorff, 2013* [4]; *M. Fromm, J. Langelage, S. Lottini, O. Philipsen, JHEP 2012* [5] ...

In the following: QCD with chemical potential (paradigmatic case).

The QCD grand canonical partition function (Wilson fermions):

$$Z = \int DU\, \mathrm{e}^{-S}, \quad S = S_{YM} - \log\det W \tag{1}$$

$$\begin{aligned} W &= 1 - \kappa \sum_{i=1}^{3} \left(\Gamma_{+i} U_{x,i} T_i + \Gamma_{-i} U^{\dagger}_{x,i} T_{-i} \right) \\ &\quad -\kappa\gamma \left(\mathrm{e}^{\mu} \Gamma_{+4} U_{x,4} T_4 + \mathrm{e}^{-\mu} \Gamma_{-4} U^{\dagger}_{x,4} T_{-4} \right) \end{aligned} \tag{2}$$

T: lattice translations, $\Gamma_{\pm\mu} = 1 \pm \gamma_\mu$, κ (hopping parameter) $\sim 1/M$.

γ: (bare) anisotropy parameter, temperature introduced as $aT = \frac{\gamma}{N_\tau}$.

For non-zero μ $\det W$ (and thus S) are complex. $\longrightarrow$ no MC!

We still have $\det W(\mu) = [\det W(-\mu)]^*$.

Attempted solutions:

1. Reweighting (RW) (the simulation produces an ensemble using only a real part of the action, the correction is done in the averages.) *I. Barbour et al (1997), Z. Fodor, S.Katz (2002)*
2. Expansion (EM) (the simulation is done at $\mu = 0$ and the averages are calculated by expanding to $\mu > 0$. *TARO (2002), Ph. De Forcrand, O. Philipsen (2002), F. Karsch et al (2004)*
3. Histogram method *S. Ejiri (2008, 2013)*, other methods
4. CLE Simulation

CLE does not suffer of overlap problem (RW) and is not restricted to small μ (EM). It can in principle work in the whole range of parameters and the ensemble is generated for the actual parameters.

But: has other problems $\longrightarrow$ understand and solve.

2. CLE: the drunkard's complex walk ...

Complex action $\longrightarrow$ complex drift $\longrightarrow$ imaginary parts for the variables

$\longrightarrow$ Process defined on the complex extension of the original manifold:

$$R^n \longrightarrow C^n \ , \ SU(n) \longrightarrow SL(n,C), \ \ldots \ .$$

The CLE with complex drift $K(z) = -\nabla_z S$

$$z(t) = x(t) + i\, y(t) \ , \ x \in \mathcal{M}_r \ , \ z \in \mathcal{M}_c \tag{3}$$

amounts to two related, real LE with independent noise terms

$$\delta z(t) = K(z,t)\, \delta t + \eta(t) \, , \quad \eta = \sqrt{N_R}\, \eta_R + \mathrm{i}\, \sqrt{N_I}\, \eta_I \tag{4}$$

$$\text{i.e. :} \qquad \delta x(t) = Re\, K(z,t)\, \delta t + \sqrt{N_R}\, \eta_R(t) \tag{5}$$

$$\delta y(t) = Im\, K(z,t)\, \delta t + \sqrt{N_I}\, \eta_I(t) \tag{6}$$

$$\langle \eta_R \rangle \ = \ \langle \eta_I \rangle = 0 \, , \quad \langle \eta_R^2 \rangle = \langle \eta_I^2 \rangle = 2\, \delta t \, , \ \langle \eta_R \eta_I \rangle = 0 \, , \quad N_R - N_I = 1$$

The processes realize a positive definite probability distribution $P(x, y)$.
Notice: $P(x, y)$ is generated at the actual values of the parameters!

Formal equivalence theorem: for analytic observables $O(x, y)$ the averages over the process reproduce the ensemble averages with the original (complex!) distribution $\rho(x) = \exp(-S(x))$:

$$\langle \mathcal{O} \rangle_{P(t)} = \langle \mathcal{O} \rangle_{\rho(t)}, \tag{7}$$

$$\langle \mathcal{O} \rangle_{P(t)} \equiv \frac{\int \mathcal{O}(x+iy) P(x,y;t) dx dy}{\int P(x,y;t) dx dy}, \quad \langle \mathcal{O} \rangle_{\rho(t)} \equiv \frac{\int \mathcal{O}(x) \rho(x;t) dx}{\int \rho(x;t) dx}. \tag{8}$$

This is what we calculate — This is what we want to get

The formal proof depends on various assumptions and can have loopholes: *some technicalities in Appendix*

Questions in controlling the process

We look for the properties of the measure ρ and of the drift K (the objects we directly have to do with) $K(z) = \partial_z \rho(z) \,/\, \rho(z)$

- There is evidence that CLE occasionally leads to wrong results.
- One can derive Consistency Conditions (CC) (combinations of the observables $\simeq$ DSE , and further bounds), not fulfilled if the process leads to wrong results.
- One can define *on-line* signals for wrong evolution.
- We have constructed *cures* for some of these problems (and work on the others!).

Notice: there are many processes $K(z)$ $(P(x, y))$ leading formally to the desired EV's. This can be used in controlling the method.

Possible sources of wrong evolution:

1. Accumulation of numerical errors. Typical effect: run-aways, divergence of some quantities. $K(z)$ becomes unbounded.
2. Unprecize sampling - in the presence of trajectories of $K(z)$ going far in the y direction.
3. Unsufficient fall off of $P(x, y)$ in the y direction - can spoil the formal proof of equivalence.
4. Non-holomorphy of the drift. Can invalidate the formal proof of equivalence. Typical for us: poles of $K(z)$ (zeroes of $\rho(z)$).

.

In some cases these effects can combine.

Cures:

Concerning the "practical problems":

1. Run-aways: efficiently eliminated by adaptive step size. Needs, however, control of the step-size dependence.

2. Unprecize sampling: constrain the distribution $P(x, y)$ by changing the process.

Concerning the "problems of principle":

3. Skirts (Unsufficient fall off of $P(x, y)$): constrain $P(x, y)$ to reduce its "skirt".

4. Meromorphic drift: need to understand when it affects the result and when not; no general method yet to handle, but partial results.

3. Tests in effective models

Meromorphic drift

Zeroes of the measure $\rightarrow$ poles of the drift (correspondingly, branch points in the effective action, *Mollgaard and Splittorff*)

From tests on simple models we found that:

- Under certain conditions zeroes of ρ may lead to sign problems.
- These problems may be countered by forcing the process to sample regions where the change of sign is taken over by the observables.
- This can be checked with reweighting procedures combined with CLE by which the wrong behaviour can be repaired. (*8.3*)
- Our ambition is, however to systematically reconstruct the CLE itself. This we did not yet achieved.
- In realistic cases (e.g., QCD) the poles do not seem to raise problems, at least in the region of physical interest.

Skirts and numerical imprecisions

In the following we shall stick to SU(3) $\longrightarrow$ SL(3,C).

The one link SU(3) reduced model

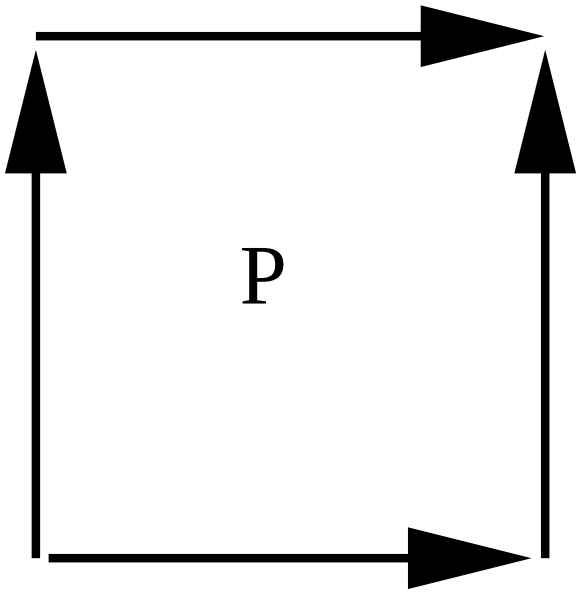

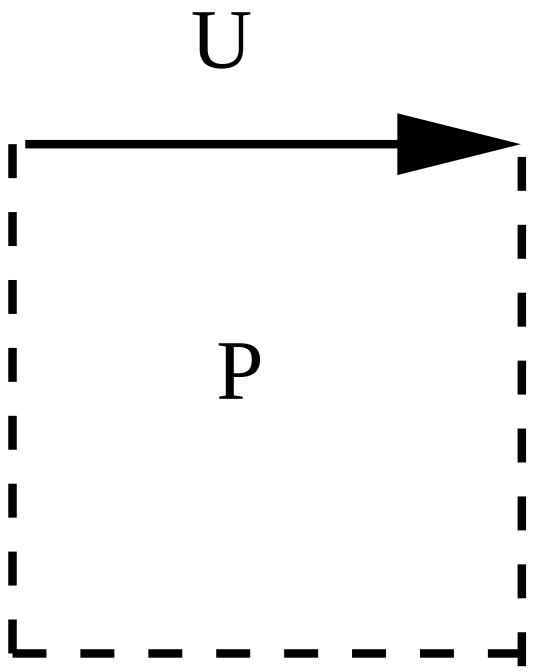

Effective model for QCD : one link in the field of its neighbors.

$$-S = \frac{\beta}{2}\left(\mathrm{tr}UA + \mathrm{tr}A^{-1}U^{-1}\right) + \ln D + \ln \tilde{D} \quad (9)$$

$$D = 1 + C\mathrm{tr}U + C^2\mathrm{tr}U^{-1} + C^3, \quad C = 2\kappa \mathrm{e}^{\mu} \quad (10)$$

$$\tilde{D} = 1 + \tilde{C}\mathrm{tr}U^{-1} + \tilde{C}^2\mathrm{tr}U + \tilde{C}^3, \quad \tilde{C} = 2\kappa \mathrm{e}^{-\mu} \quad (11)$$

The matrices $A \in GL(3, C)$ simulate the stapples.

Diagonalize $A = V^{-1}BV \longrightarrow$

$$-S_Y = \frac{\beta}{2}\left(\mathrm{tr}\hat{U}B + \mathrm{tr}B^{-1}\hat{U}^{-1}\right), \; B = \mathrm{diag}(\alpha_1, \alpha_2, \alpha_3), \; \hat{U} = VUV^{-1}$$

Invariance of the Haar measure $\longrightarrow$ new variables $\hat{U} \in SL(3, C)$
(the determinant is invariant under this transformation).

"Cartan" reduction: explicit integration in the 3 complex angles on the diagonal, with the reduced Haar measure $H \longrightarrow$ effective model:

$$-S = \frac{\beta}{2}\sum_{i=1}^{3}\left(\alpha_i e^{iw_i} + \alpha_i^{-1} e^{-iw_i}\right) + \ln D + \ln \tilde{D} + f \ln H \tag{12}$$

$$H = \sin^2\frac{w_2 - w_3}{2}\sin^2\frac{w_3 - w_1}{2}\sin^2\frac{w_1 - w_2}{2},\ w_1 + w_2 + w_3 = 0$$

Effect of the neighbors: coded in the complex coefficients α.

Observables and CC conditions :

$$O_n = \mathsf{tr}(\hat{U}^n) = \mathrm{e}^{i\,nw_1} + \mathrm{e}^{i\,nw_2} + \mathrm{e}^{i\,nw_3} \tag{13}$$

$$E_n = \left(\nabla^2 + K\nabla\right) O_n,\ K = -\nabla S \tag{14}$$

The process runs in three or (equivalently) two angles, with correspondingly three (two) noise terms.

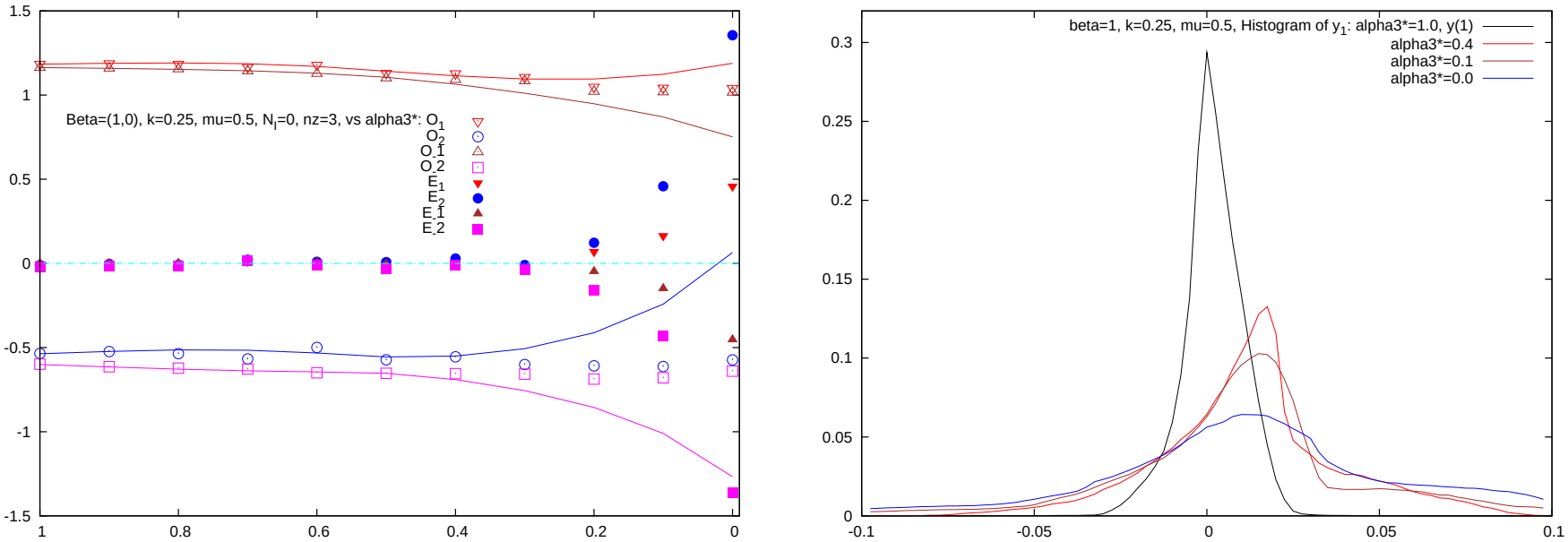

Figure 2: Effective model. *Left*: Dependence of the observables and the CC's on $\mathrm{Re}\,\alpha_3$ ($\mathrm{Im}\,\alpha_3$ increases correspondingly). The violation of the CC's signalizes discrepant results. *Right*: Histograms of the equilibrium measure for different $\mathrm{Re}\,\alpha_3$. Discrepant results corrrelate with wide skirts of the distributions.

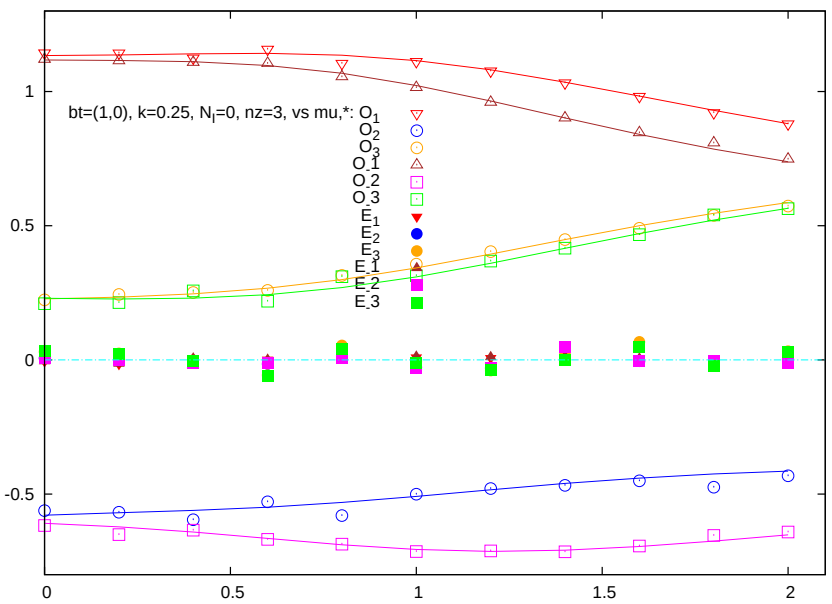

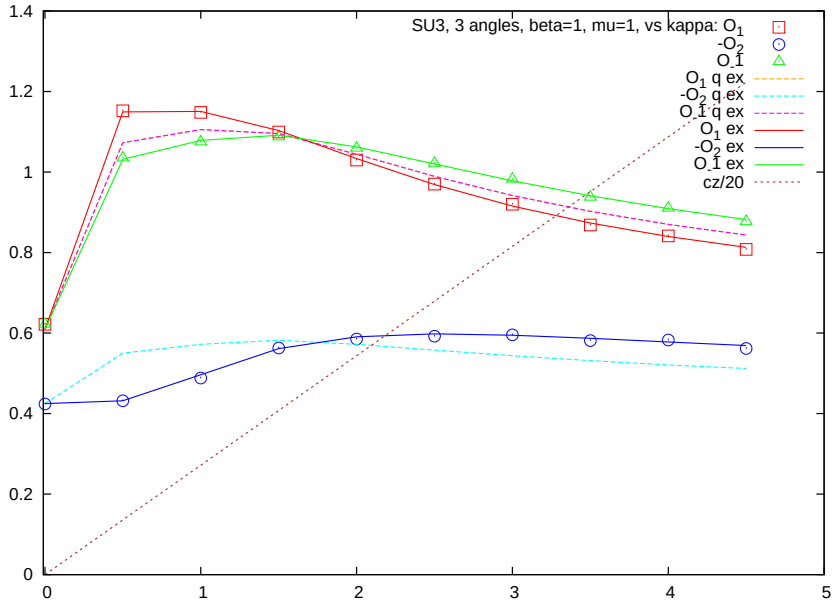

Figure 3: Effective model, $\alpha = 1$. *Left*: Dependence of the observables and the CC's on μ. *Right* Dependence of the observables on κ.

The Polyakov chain

Many variables (as in lattice theory): closed Polyakov line with n links.

The model is soluble (gauge transformation to 1 link model), but the process is done in n links.

Action :

$$-S = (\beta + 2\,\kappa \mathrm{e}^{\mu})\, Tr\,(U_1 \cdots U_n) + (\beta + 2\,\kappa \mathrm{e}^{-\mu})^*\, Tr\,\left(U_n^{-1} \cdots U_1^{-1}\right)$$

The process runs in all 8 (complex) angles, with real noise:

$$\Delta A^a_{i,\mu} = \epsilon K^a_{i,\mu}(U) + \sqrt{\epsilon}\,\eta\ , \quad U_{i,\mu} \longrightarrow \mathrm{e}^{i\,\sum_a \lambda_a\,\Delta A^a_{i,\mu}}\, U_{i,\mu} \tag{15}$$

We observe wrong evolution setting in for large n even for values of the parameters for which at $n = 1$ everything works fine!

We learn from these exercises that:

- Wide skirts of the distributions (far diffusing scatter plots) lead to wrong results.
- These effects apparently come from
  - incorrect sampling and accumulation of numerical errors
  - violation of the equivalence proof by boundary terms.
- For *gauge theories* a clear signal of wrong evolution is *uncontrolled departure* from the unitary manifold.
- This suggests using *gauge symmetry* to redesign the process such that it stays as near as possible to the unitary manifold.

4. Gauge cooling

For a correctly evolving process a "unitarity norm" such as $trU\,U^\dagger - 3$ should *converge* to some (generally non-zero) value.

Since the clear symptom of incorrect evolution is the *divergence* of the unitarity norm (*UN*) we introduce a gauge cooling to minimize the unitarity norm

$$UN \equiv \sum_{links} \left[\frac{1}{2} tr \left(U\,U^\dagger + U^{-1}\,U^{-1\,\dagger} \right) - 3 \right] \tag{16}$$

This succeeds by successive gauge transformations of the links

$$R_k = e^{i\alpha\,\epsilon\,dS_G} \;,\; U_k \longrightarrow R_k\,U_k \;,\; U_{k-1} \longrightarrow U_{k-1} R_k^{-1}$$

- dS_G: the gradient of the UN
- α: the strength of the *gauge force*, ϵ: step size.

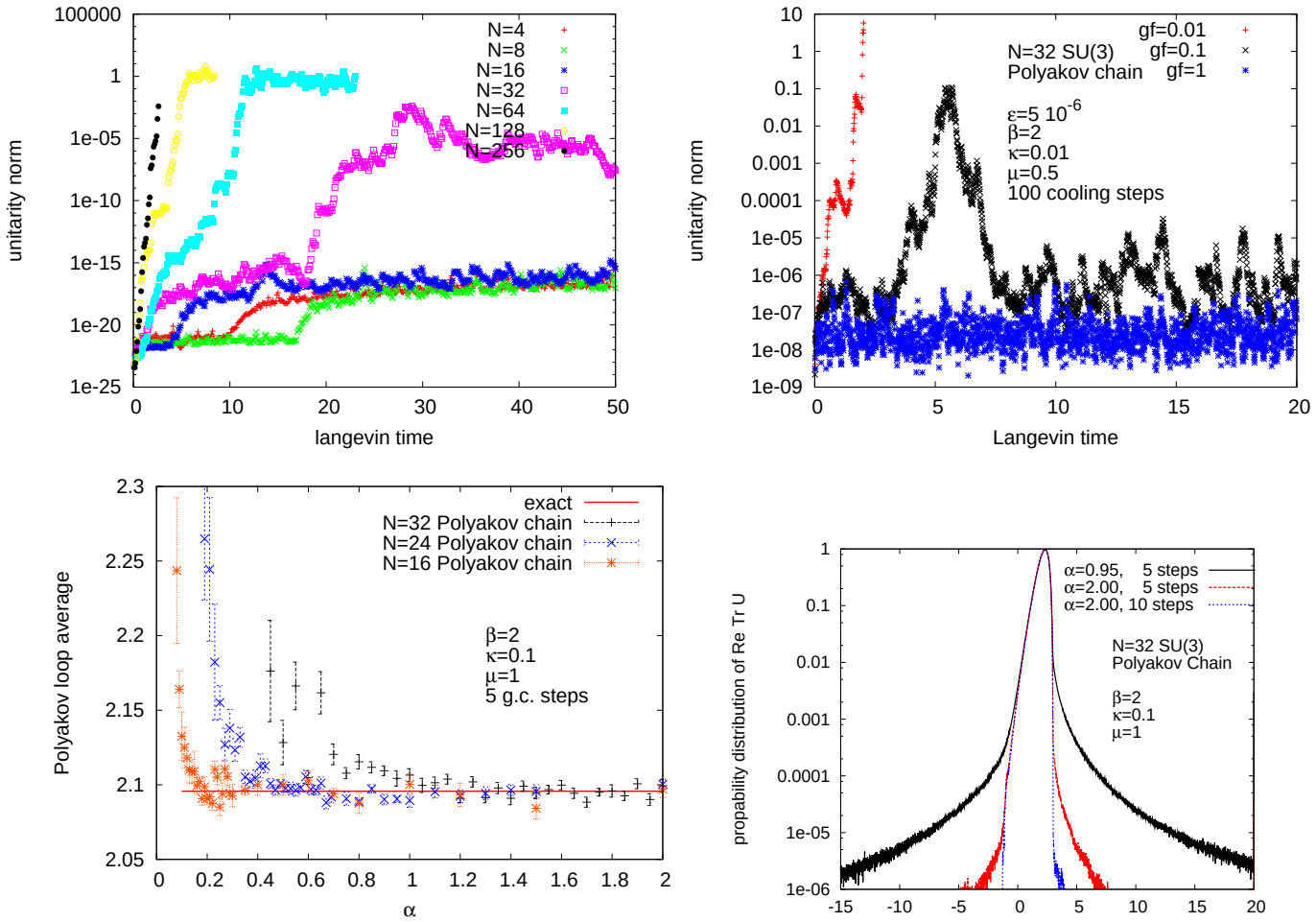

Figure 4: Polyakov chain. Upper plots: evolution of the *UN*, *Left*: euclidean case, various n, little cooling; *Right*: complex case, various amount of cooling. Lower plots: Observables and distributions for various amount of cooling.

Notice:

- Gauge Cooling is a general method for gauge theories.
- It modifies the CLE process. It can be realized as intermittent gauge transformations or as additional drift $along$ the gauge orbits - akin with stochastic gauge fixing.
- It does not change the observables but $"repairs"$ the process, that is, the sampling of the observables.
- It must not be confused with usual cooling, since it does not change gauge independent quantities, in particular the action.

5. Lattice QCD with chemical potential, HD approximation, Wilson fermions

The lattice HDMQCD model *I. Bender, T. Hashimoto, F. Karsch, V. Linke, A. Nakamura, M. Plewnia, IOS, W. Wetzel,* KEK 1991! relies on the *hopping parameter expansion* of the determinant.

In the limit $\kappa \to 0,\ \mu \to \infty,\ \ \zeta = \kappa\, \mathrm{e}^{\mu}\ : fixed$

only the Polyakov loops survive and the determinant factorizes.

Higher orders: κ^2 , κ^4 : straightforward (but beware combinatorics!).

HDM-QCD and HDQCD (symmetrized HDM) applications:

- Explicit formulae, extensive calculations, (full Y-M action, refined reweighting), *R. De Pietri, A. Feo, E. Seiler, IOS, PRD 2007*
- Strong coupling expansion for the Y-M action, reweighting and CLE *P. de Forcrand, M. Fromm, PRL 2010, M. Fromm, J. Langelage, S. Lottini, M. Neuman, O. Philipsen, PRL 2012*
- CLE and refined reweighting, full Y-M action *E. Seiler, D. Sexty, IOS, PLB 2013*

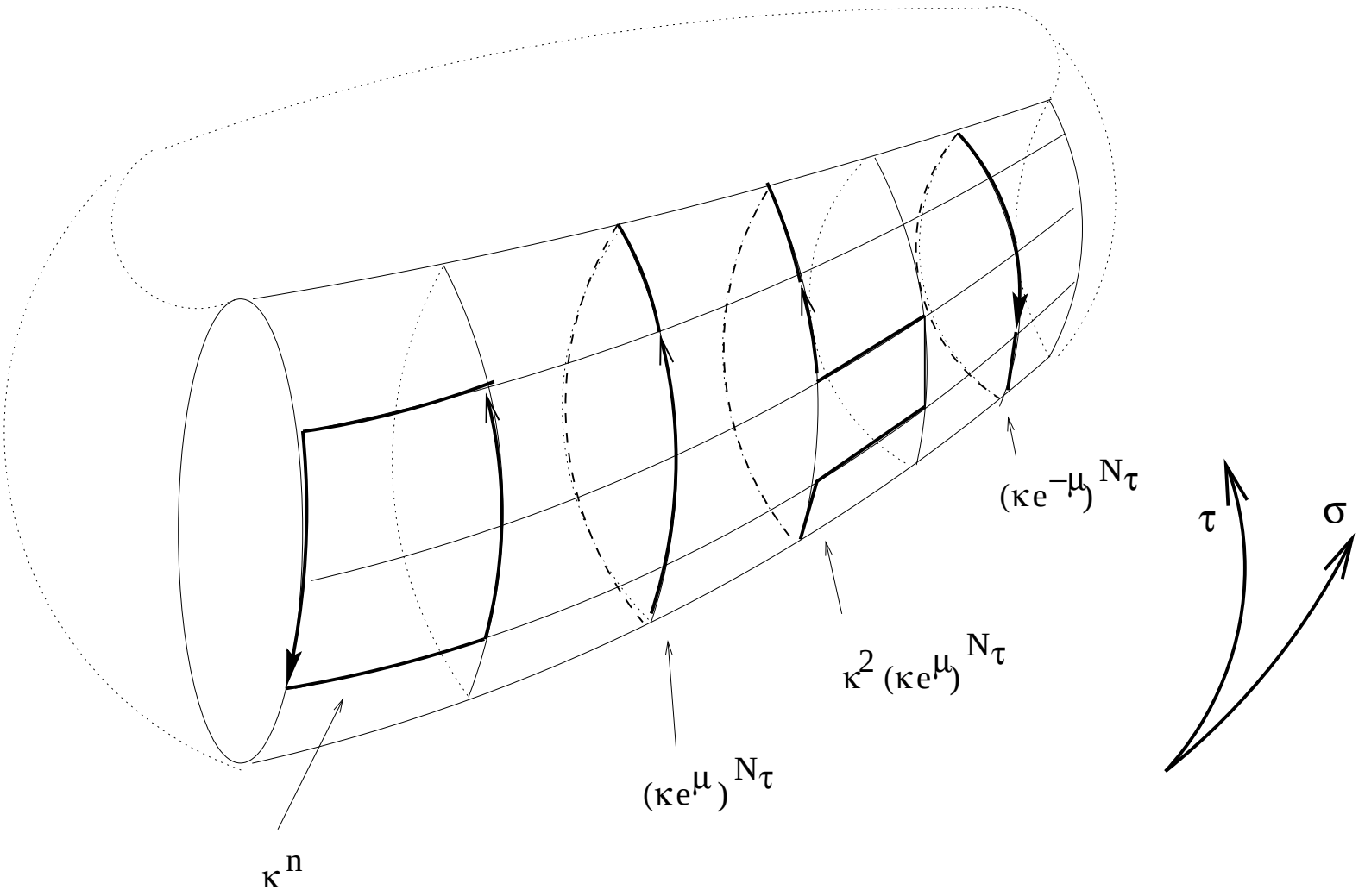

$$T = 1 / N_\tau a_\tau$$

Figure 5: The HDM - QCD model: 0-th and 2-nd order.

HDQCD ("symmetrized" HDM), Wilson fermions

Action and observables (pbc/apbc):

$$S = \frac{\beta}{6} S_{YM}(\{U\}) + \ln\det \mathbf{M}(\mu) \tag{17}$$

$$\det \mathbf{M}(\mu) \equiv \prod_x \mathrm{Det}\left(1 + C\mathcal{P}_x\right)^2 \mathrm{Det}\left(1 + C'\mathcal{P}_x^{-1}\right)^2 \tag{18}$$

$$\mathrm{Det}\left(1 + C\mathcal{P}_x\right)^2 = (1 + C^3 + 3CP_x + 3C^2 P'_x)^2 \tag{19}$$

$$C = [2\kappa \exp(\mu))]^{N_t} \ , \ C' = [2\kappa \exp(-\mu)]^{N_t} \tag{20}$$

$$\mathcal{P}_x \ = \ \prod_{\tau=0}^{N_\tau - 1} U_{x+r\hat{0},0} \ , \ P_x = \frac{1}{3}\mathrm{tr}\,\mathcal{P}_x; \quad P'_x = \frac{1}{3}\mathrm{tr}\,\mathcal{P}_x^{-1} \, . \tag{21}$$

We measure also plaquettes, density and the average phase factor

$$\langle n \rangle = \frac{1}{V}\frac{\partial \ln Z}{\partial \mu}, \quad \left\langle e^{2i\phi} \right\rangle \equiv \left\langle \frac{\det \mathbf{M}(\mu)}{\det \mathbf{M}(-\mu)} \right\rangle \tag{22}$$

We observe the same behaviour as in the Polyakov chain model. The effect of cooling is dramatic.

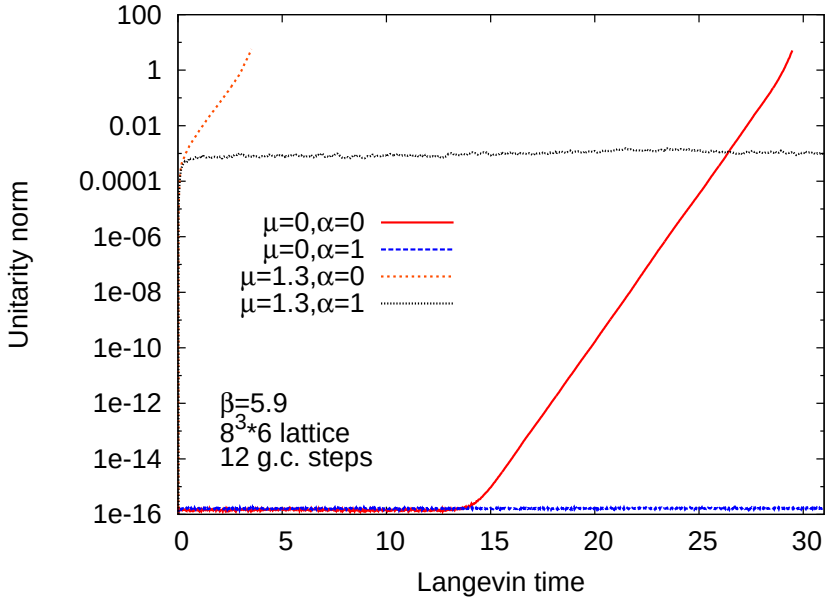

Figure 6: HDQCD: evolution of the unitarity norm with and without g.c. for $\beta = 5.9$, $8^3 \times 6$ lattice.

CLE for HDQCD using long cooling.

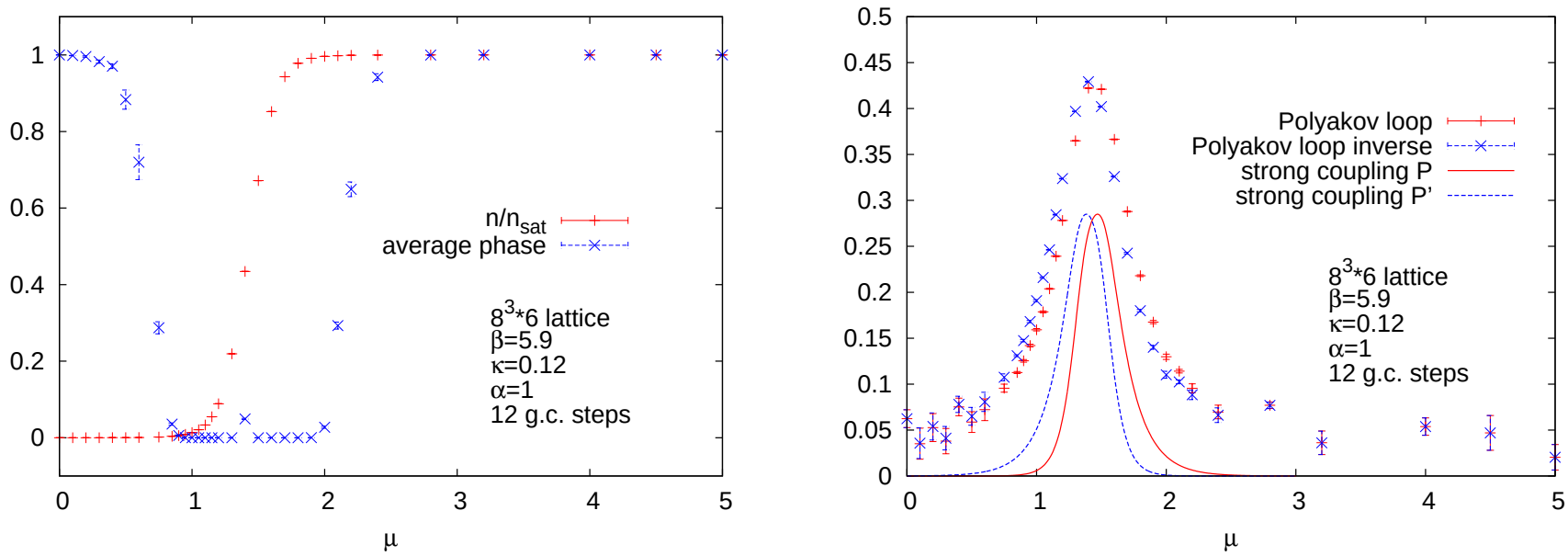

Figure 7: HDQCD. *Left*: Baryon density and average phase for $\beta = 5.9$, $8^3 \times 6$ lattice. *Right*: $\langle \mathcal{P} \rangle$, $\langle \mathcal{P}' \rangle$ vs. μ at $\beta = 5.9$ on a $8^3 \times 6$ lattice; solid lines: analytic strong coupling result.

HDQCD, comparison CLE with Reweighting (RW).

For Reweighting we employ a refined procedure ($De\ Pietri\ et\ al,\ with\ symmetrized\ action$) which uses a positive real factor in the Boltzmann factor and thus partly accounts for the chemical potential dependence in producing the ensemble.

The rest of the Boltzmann factor is taken care of, as usual, in the averages.

In this way one can extend to some extent the limitations in the parameters typical to RW methods.

This permits using these calculations for comparisons with CLE .

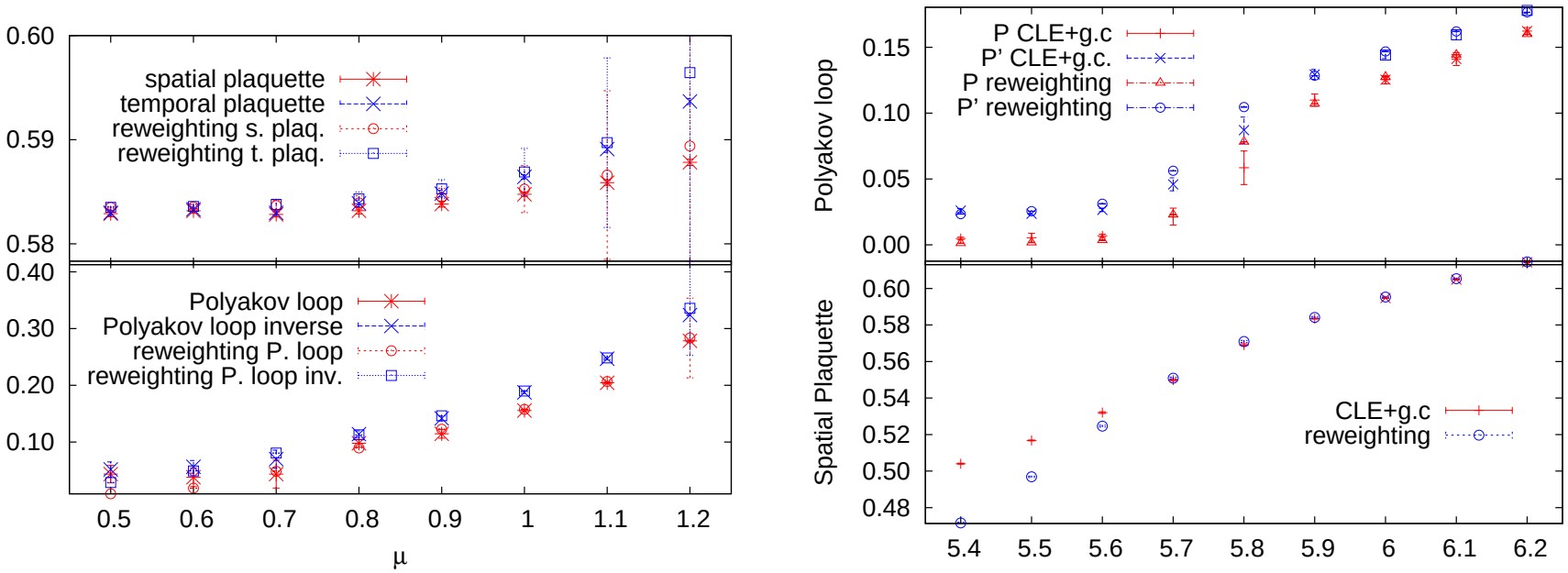

Figure 8: HDQCD: $\langle P \rangle$, $\langle P' \rangle$ and plaquettes for RW *and* CLE (6^4 lattice, $\alpha = 1$, 12 g.c. steps, adaptive step size) at $\beta = 5.9$ vs μ (*left*) and at $\mu = 0.85$ vs β (*right*). Large errors only affect RW at large μ.

Generally very good agreement, only discrepancy in the plaquettes below $\beta \sim 5.6$.

The *deterioration threshold at* $\beta \sim 5.6$ appear to be independent on the lattice size and only weakly dependent on μ, and thus stay well below the phase transition on large lattices. A continuum limit would thus be safe both in the deconfined and in the confined phase.

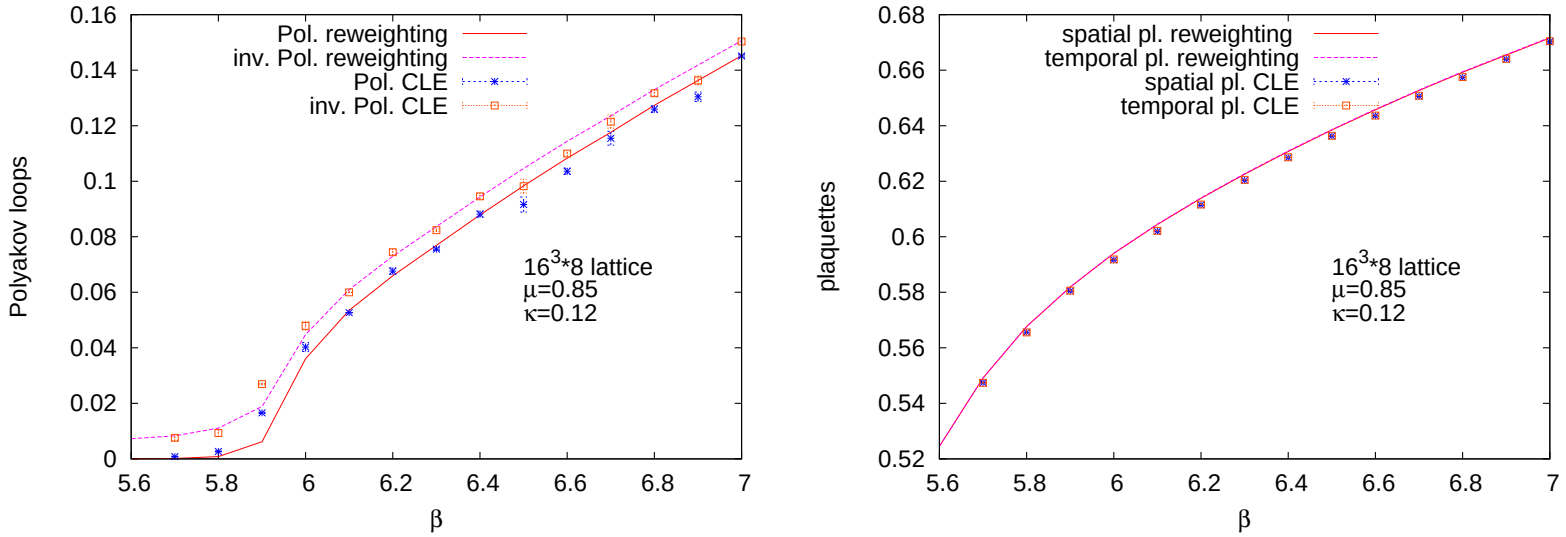

Figure 9: HDQCD: CLE and RW on $16^3.8$ lattices, Polyakov loops (*left*) and plaquettes (*right*). An apparent small shift may be due to finite step effects.

6. Full Lattice QCD with chemical potential, staggered fermions

Staggered QCD action and the CLE process:

$$S_{eff}[U] = S_g[U] - \frac{N_F}{4}\ln\det M(\mu,U) \tag{23}$$

$$\begin{aligned} M(\mu,U)_{xy} &= m\delta_{xy} + \sum_\nu \frac{\eta_\nu(x)}{2a}\left[e^{\delta_{\nu 4}\mu}U_\nu(x)\delta_{x+a_\nu,y}\right. \\ &\quad \left. - e^{-\delta_{\nu 4}\mu}U_\nu^{-1}(x-a_\nu)\delta_{x-a_\nu,y}\right], \end{aligned} \tag{24}$$

$$\epsilon_x M(\mu,U)_{xy}\epsilon_y = M^\dagger(-\mu^*,U)_{yx}, \quad \epsilon_x = (-1)^{x_1+x_2+x_3+x_4}$$

with $\eta_\mu(x)$: the staggered signs, and (a)pbc.

The CLE updating is defined as before, with the drift

$$K_{ax\nu} = -D_{ax\nu}S_g[U] + \frac{N_F}{4}\mathrm{T}r[M^{-1}(\mu,U)D_{ax\nu}M(\mu,U)] \tag{25}$$

In full QCD as in HDQCD gauge cooling is essential, already at $\mu = 0$.

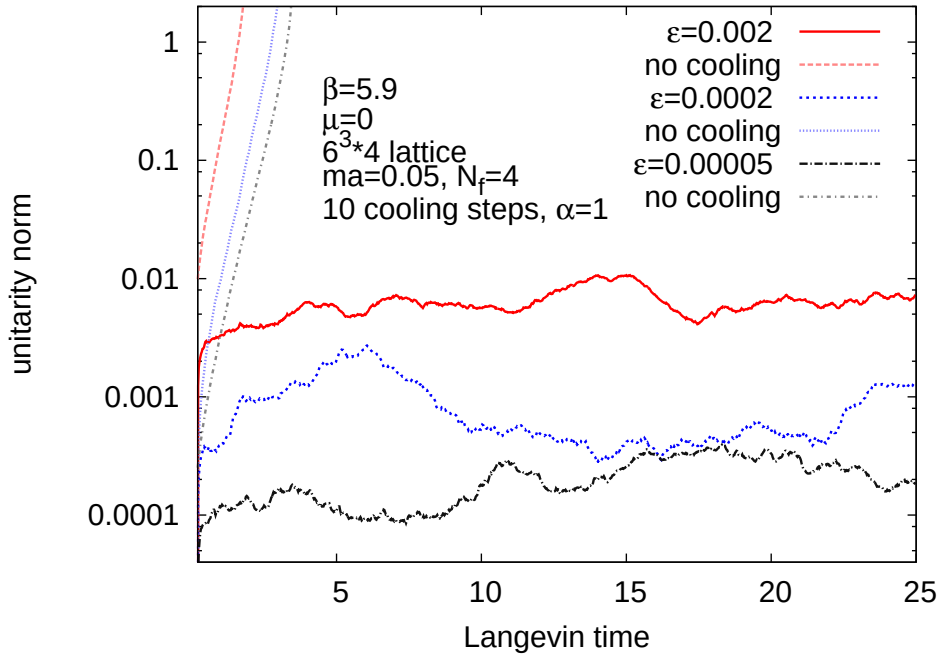

Figure 10: Unitarity norm as a function of Langevin time with and without cooling for several values of the Langevin timestep ϵ.

Results for QCD at $\mu > 0$, small fermion mass.

D. Sexty, PLB 2014, to appear

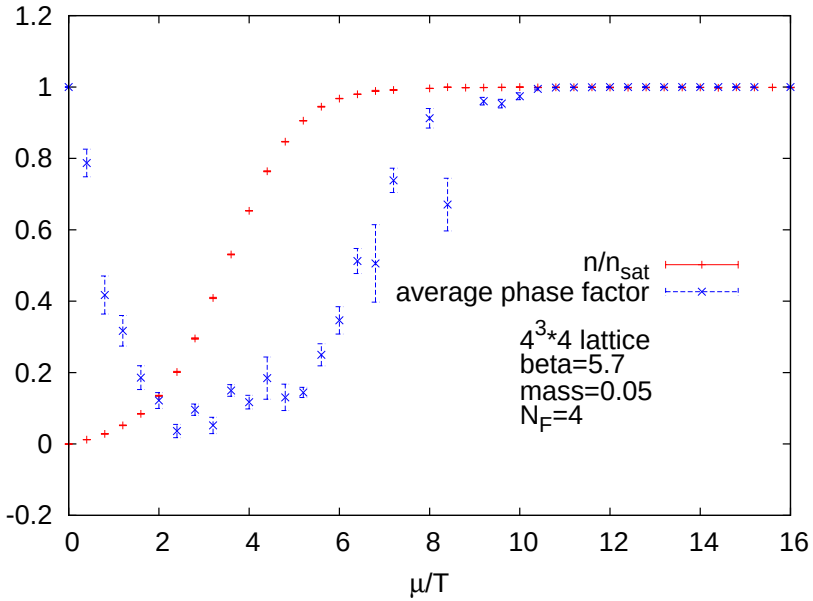

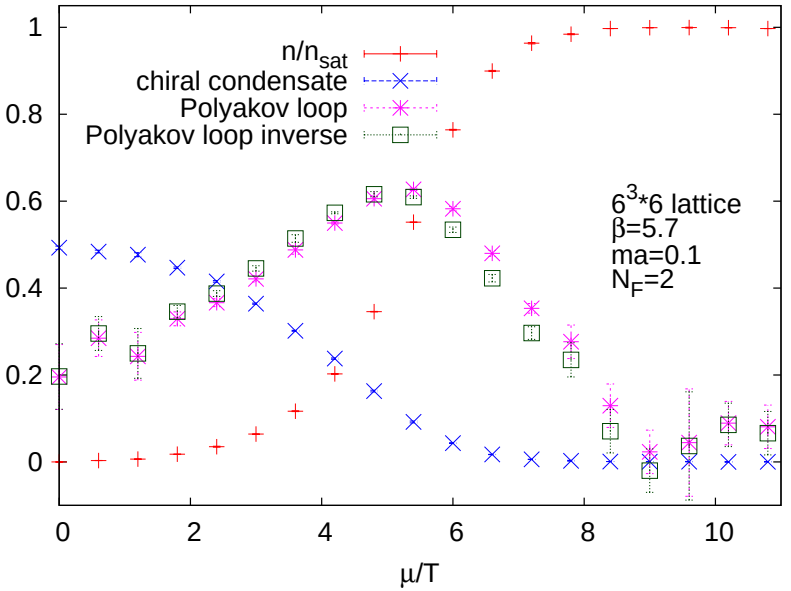

Figure 11: Average phase factor and density, 4^4 lattice (*left*) and density, chiral condensate and Polyakov loops, 6^4 lattice (*right*) vs μ/T.

Full QCD, comparison with *multi-parameter reweighting*

S. Borsanyi, Z. Fodor, S. Katz, D. Sexty (in preparation)

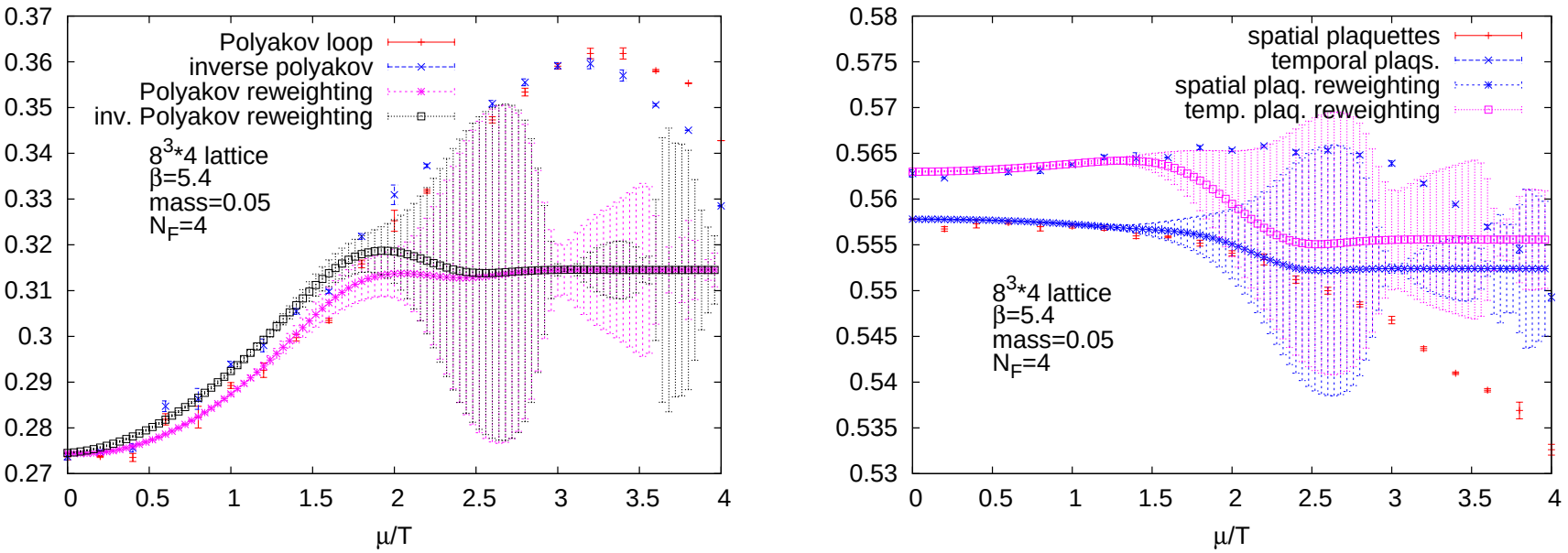

Figure 12: Polyakov loops (*left*) and plquettes (*right*) vs μ/T, $8^3.4$ lattice, comparison with full QCD reweighting.

The results agree very well, but at higher μ the reweighting has prohibitive errors while CLE remains stable.

Full QCD, comparison with HQCD *D. Sexty, PLB 2014*

The comparison is done for 1 flavour, full QCD with staggered and HDQCD with Wilson fermions with the identification $m = 1/(4\kappa)$

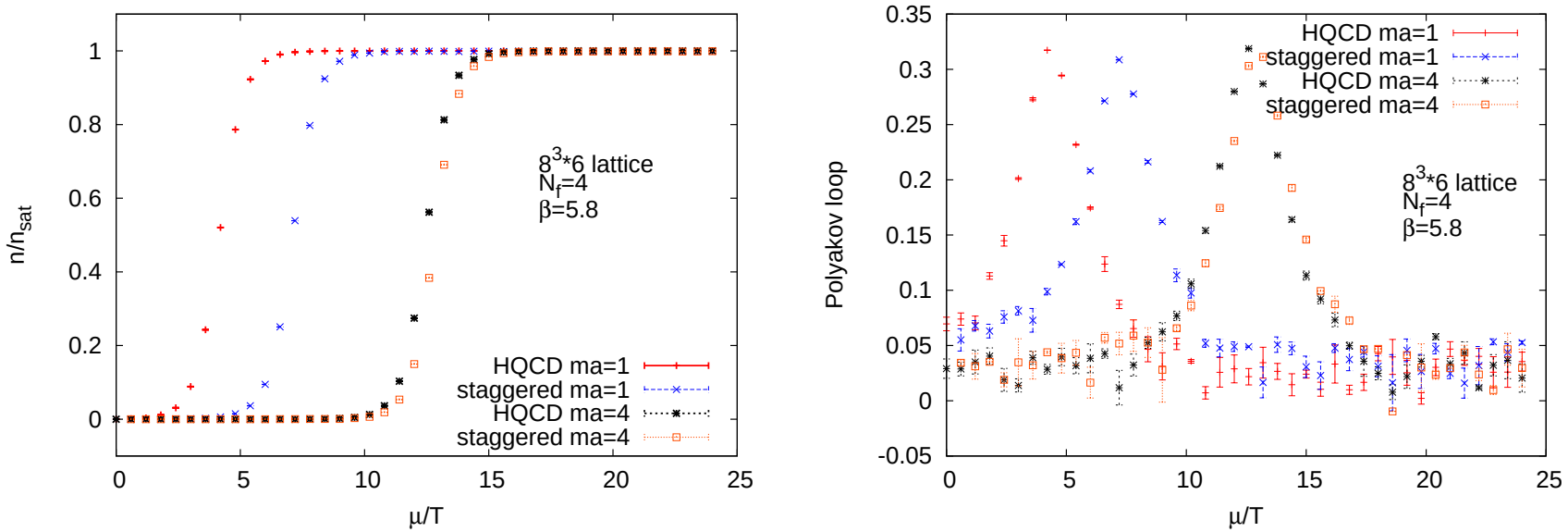

Figure 13: Comparison of the average densities (*left*) and Polyakov loops (*right*) measured in HQCD and in full QCD with staggered fermions.

HDQCD agrees very well to full QCD at large fermion mass, but the qualitative behaviour appears very similar also at intermediate mass!

7. Discussion

- CLE has the chance to become a versatile, general method for solving the problem of complex action (QCD with chemical potential, non-equilibrium QFT and real time evolution, etc).
- The method does not suffer of cancellations and of the overlap problem.
- The method works in a parameter range not reached by any other method.
- The volume dependence is comparable with that of MC for real action (and differs essentially from that of RW).

Insights and solutions:

- Some problems seem to originate from a combination of the particularities of the evolution (fixed point structure, etc) and of numerical imprecisions.
- We could relate these problems to the behaviour of the distribution in the imaginary direction and solve them for gauge theories using the gauge symmetry (gauge cooling).
- A possible source of trouble, not yet solved in principle are poles in the drift. In realistic, interesting cases this does not seem to have significant effects and by smoothing out the configurations gauge cooling may help also here. Nevertheless we want to find a systematic understanding.
- CLE with gauge cooling allowed us to analyze full QCD in the whole region of interest aiming at physical results far beyond the reach of any other method.

8. Appendix

1. Bibliography
2. Some technicalities
3. Test for poles
4. Effective model
5. Hopping parameter expansion
6. Random Walk for CLE
7. Staggered determinant in full QCD
8. More figures ...

8.1 Bibliography

References

[1] P. de Forcrand, PoS LAT **2009**, 010 (2009) [arXiv:1005.0539]; G. Aarts, PoS LATTICE **2012** (2012) 017 [arXiv:1302.3028].

[2] G. Parisi, Phys. Lett. **131 B** (1983) 393.

[3] G. Aarts and I. -O. Stamatescu, JHEP **0809** (2008) 018 [arXiv:0807.1597].

[4] G. Aarts, Phys. Rev. Lett. **102** (2009) 131601 [arXiv:0810.2089 [hep-lat]].

[5] G. Aarts and K. Splittorff, JHEP **1008**, 017 (2010) [arXiv:1006.0332 [hep-lat]].

[6] G. Aarts and F. A. James, JHEP **1201** (2012) 118 [arXiv:1112.4655].

[7] E. Seiler, D. Sexty and I. -O. Stamatescu, Phys. Lett. B **723**, 213

(2013) [arXiv:1211.3709 [hep-lat]].

[8] J. Ambjorn and S. K. Yang, Phys. Lett. B **165**, 140 (1985).

[9] J. Ambjorn, M. Flensburg and C. Peterson, Nucl. Phys. B **275**, 375 (1986).

[10] G. Aarts and F. A. James, JHEP **1008** (2010) 020 [arXiv:1005.3468].

[11] J. M. Pawlowski and C. Zielinski, Phys. Rev. D **87**, 094509 (2013) [arXiv:1302.2249 [hep-lat]].

[12] J. M. Pawlowski and C. Zielinski, Phys. Rev. D **87**, 094503 (2013) [arXiv:1302.1622 [hep-lat]].

[13] J. Berges and I. -O. Stamatescu, Phys. Rev. Lett. **95** (2005) 202003 [hep-lat/0508030].

[14] J. Berges, S. .Borsanyi, D. Sexty and I. -O. Stamatescu, Phys. Rev. D **75** (2007) 045007 [hep-lat/0609058].

[15] J. Berges and D. Sexty, Nucl. Phys. B **799** (2008) 306 [arXiv:0708.0779].

[16] L. Bongiovanni, G. Aarts, E. Seiler, D. Sexty and I. -O. Stamatescu, arXiv:1311.1056 [hep-lat].

[17] G. Aarts, E. Seiler and I. -O. Stamatescu, Phys. Rev. D **81** (2010) 054508 [arXiv:0912.3360]; G. Aarts, F. A. James, E. Seiler and I. -O. Stamatescu, Eur. Phys. J. C **71** (2011) 1756 [arXiv:1101.3270].

[18] C. Pehlevan and G. Guralnik, Nucl. Phys. B **811** (2009) 519 [arXiv:0710.3756]; G. Guralnik and C. Pehlevan, Nucl. Phys. B **822** (2009) 349 [arXiv:0902.1503].

[19] G. Aarts, F. A. James, J. M. Pawlowski, E. Seiler, D. Sexty and I. -O. Stamatescu, JHEP **1303**, 073 (2013) [arXiv:1212.5231 [hep-lat]].

[20] A. Duncan and M. Niedermaier, Annals Phys. **329**, 93 (2013).

[21] G. Aarts, P. Giudice and E. Seiler, arXiv:1306.3075 [hep-lat].

[22] A. Mollgaard and K. Splittorff, arXiv:1309.4335 [hep-lat].

[23] G. G. Batrouni, G. R. Katz, A. S. Kronfeld, G. P. Lepage, B. Svetitsky and K. G. Wilson, Phys. Rev. D **32** (1985) 2736.

[24] M. Fukugita, Y. Oyanagi and A. Ukawa, Phys. Rev. D **36** (1987) 824.

[25] D. Zwanziger, Nucl. Phys. B **192** (1981) 259; P. Rossi, C. T. H. Davies and G. P. Lepage, Nucl. Phys. B **297** (1988) 287.

[26] G. Aarts, L. Bongiovanni, E. Seiler, D. Sexty and I. -O. Stamatescu, arXiv:1303.6425 [hep-lat].

[27] T. D .Cohen, Phys. Rev. Lett. **91** (2003) 222001 [hep-ph/0307089].

[28] I. Bender, T. Hashimoto, F. Karsch, V. Linke, A. Nakamura, M. Plewnia, I. O. Stamatescu and W. Wetzel, Nucl. Phys. Proc. Suppl. **26** (1992) 323; T. C. Blum, J. E. Hetrick and D. Toussaint, Phys. Rev. Lett. **76** (1996) 1019 [hep-lat/9509002]

[29] R. De Pietri, A. Feo, E. Seiler and I. -O. Stamatescu, Phys. Rev. D **76** (2007) 114501 [arXiv:0705.3420].

[30] M. Fromm, J. Langelage, S. Lottini and O. Philipsen, JHEP **1201** (2012) 042 [arXiv:1111.4953]; M. Fromm, J. Langelage, S. Lottini, M. Neuman and O. Philipsen, from the lattice," arXiv:1207.3005 [hep-lat].

[31] P. de Forcrand and M. Fromm, Phys. Rev. Lett. **104** (2010) 112005 [arXiv:0907.1915 [hep-lat]].

[32] S. Borsányi, Z. Fodor, S.D. Katz, D. Sexty, in preparation.

[33] J. Flower, S. Otto, S. Callahan, Phys.Rev.D34:598,1986.

Some publications in our group, various combinations:

- Lattice simulations of real-time quantum fields, J. Berges, Sz. Borsanyi, D. Sexty, I.-O. S.
- Stochastic quantization at finite chemical potential, G. Aarts, I.-O. S.
- The Complex Langevin method: When can it be trusted? G. Aarts, E. Seiler, I.-O. S.
- Complex Langevin: Etiology and Diagnostics of its Main Problems, G. Aarts, F. A. James, E. Seiler, I.-O. S.
- Complex Langevin dynamics: criteria for correctness, G. Aarts, F. A. James, E. Seiler, I.-O. S.
- Complex Langevin dynamics in the SU(3) spin model at nonzero chemical potential revisited, G. Aarts, F. A. James

- Stability of complex Langevin dynamics in effective models G. Aarts, F. A. James, J.. Pawlowski, E. Seiler, D. Sexty, I.-O. S.
- Gauge cooling in complex Langevin for QCD with heavy quarks, E. Seiler, D. Sexty, I.-O. S.
- Controlling complex Langevin dynamics at finite density, G. Aarts, L. Bongiovanni, E. Seiler, D. Sexty, I.-O. S.
- Adaptive gauge cooling for complex Langevin dynamics, G. Aarts, L. Bongiovanni, E. Seiler, D. Sexty, I.-O. S.
- Localised distributions and criteria for correctness in complex Langevin dynamics, G. Aarts, P. Giudice, E. Seiler - Simulating full QCD at nonzero density using complex Langevin equation D. Sexty

8.2 Some technicalities

Observables and distributions.

Consider an "observable" $\mathcal{O}$: an analytic function on $\mathcal{M}_c$.

The expectation values are averages over the noise. We have:

$$\partial_t \langle \mathcal{O}(z(t)) \rangle = \langle L\, \mathcal{O}(z(t)) \rangle = \langle \tilde{L}\, \mathcal{O}(z(t)) \rangle \tag{26}$$

$$L = [N_R \nabla_x + K_x]\, \nabla_x + [N_I \nabla_y + K_y]\, \nabla_y \tag{27}$$

$$\tilde{L} = [\nabla_z + K(z)]\, \nabla_z \tag{28}$$

(the second equality in Eq.(26) follows from the C-R conditions).

Notice that L explicitely involves N_R, N_I while $\tilde{L}$ does not.

Notice: the following considerations assume holomorphy of the drift and of the observables.

We can define a FPE for the *probability distribution* $P(x,y,t)$ as realized in the process (5,6) on $\mathcal{M}_c$:

$$\partial_t P(x,y,t) = L^T\, P(x,y,t), \quad \langle P, L\,\mathcal{O}\rangle = \langle L^T P, \mathcal{O}\rangle, \tag{29}$$

$$L^T = [\nabla_x\,(N_R\,\nabla_x - ReK(z)) + \nabla_y\,(N_I\,\nabla_y - ImK(z))] \tag{30}$$

We can also define a FPE for a complex *"distribution"* $\rho(x)$ on $\mathcal{M}_r$:

$$\partial_t \rho(x,t) = L_0^T\,\rho(x,t), \quad L_0^T = \nabla_x\,(\nabla_x - K) \tag{31}$$

which has as (complex) stationary solution $\rho(x;\infty) \propto \exp[-S(x)]$.

We can thus define two types of expectation values

$$\langle\mathcal{O}\rangle_{P(t)} \equiv \frac{\int \mathcal{O}(x+iy)P(x,y;t)dxdy}{\int P(x,y;t)dxdy}, \quad \langle\mathcal{O}\rangle_{\rho(t)} \equiv \frac{\int \mathcal{O}(x)\rho(x;t)dx}{\int \rho(x;t)dx} \tag{32}$$

and what we should like to show (for large t) is

$$\langle\mathcal{O}\rangle_{P(t)} = \langle\mathcal{O}\rangle_{\rho(t)}, \tag{33}$$

Set up for the correctness question.

Instead of evolving $P(x, y, t)$ we evolve the observables.
For analytic functions we can use interchangeably L and $\tilde{L}$:

$$\partial_t \mathcal{O}(z;t) = \tilde{L}\mathcal{O}(z;t) \quad (t \geq 0) \rightarrow \ \mathcal{O}(z;t) = \exp[t\,\tilde{L}]\mathcal{O}(z). \tag{34}$$

or equivalently

$$\partial_t \mathcal{O}(x;t) = L_0\mathcal{O}(x;t) \quad (t \geq 0) \rightarrow \ \mathcal{O}(x;t) = \exp[t\,L_0]\mathcal{O}(x). \tag{35}$$

We consider the interpolation

$$F_{\mathcal{O}}(t,\tau) \ \equiv \ \int P(x,y;t-\tau)\mathcal{O}(x+iy;\tau)dxdy, \tag{36}$$

$$F_{\mathcal{O}}(t,0) \ = \ \langle \mathcal{O} \rangle_{P(t)}, \quad F_{\mathcal{O}}(t,t) = \langle \mathcal{O} \rangle_{\rho(t)}. \tag{37}$$

Proof of the first equality: self evident.

Proof of the second equality:

$$\begin{aligned} F_{\mathcal{O}}(t,t) &= \int P(x,y;0)\left(e^{tL}\mathcal{O}\right)(x+iy;0)dxdy \\ &= \int \rho(x;0)\left(e^{tL_0}\mathcal{O}\right)(x;0)dx \\ &= \int \mathcal{O}(x;0)\left(e^{tL_0^T}\rho\right)(x;0)dx \\ &= \langle \mathcal{O} \rangle_{\rho(t)}, \end{aligned} \tag{38}$$

Here we set $P(x,y;0) = \rho(x;0)\,\delta(y)$ with a suitable $\rho(x;0)$ as initial conditions and used partial integration in x which is unproblematic (x will normally be a compact variable).

Formal proof of correctness and its loophole.

Equality $\langle \mathcal{O} \rangle_{P(t)} = \langle \mathcal{O} \rangle_{\rho(t)}$ is ensured if $F_{\mathcal{O}}(t, \tau)$ is independent of τ:

$$\frac{\partial}{\partial \tau} F_{\mathcal{O}}(t, \tau) = - \int \left(L^T P(x, y; t - \tau) \right) \mathcal{O}(x + iy; \tau) dx dy + \int P(x, y; t - \tau) L \mathcal{O}(x + iy; \tau) dx dy. \quad (39)$$

The RHS =0 after integration by parts.

This proof relies on neglecting boundary terms from the y-integration.

Loophole: The proof fails if the fall off of the probability distribution is not sufficient for the boundary terms to vanish.

8.3

One U(1) link integral with "determinant" factors.

(For another soluble model: Random matrices *K.Splittorff.*)

$$\rho(z) = \prod_i D_i(z)\, \mathrm{e}^{\beta\, \cos(z)}, \tag{40}$$

$$D_i(z) = (1 + \kappa_i \cos(z - i\,\mu_i))^{f_i}\,, \tag{41}$$

$$K(z) = -\beta\, \sin(z) - \sum_i f_i\, \kappa_i\, \frac{\sin(z - i\,\mu_i)}{1 + \kappa_i \cos(z - i\,\mu_i)} \tag{42}$$

The drift has poles:

$$\kappa_i \geq 1: \;\; \cos(x) = -\frac{1}{\kappa_i}, \qquad y = \mu_i\,; \qquad res = f_i \tag{43}$$

$$\kappa_i < 1: \;\; x = \pi, \quad \cosh(y - \mu_i) = \frac{1}{\kappa_i}\,; \quad res = f_i \tag{44}$$

Since ρ has zeroes we can speak of a sign problem. (Different concept!)

For real models with sign problem the process can be shown to separate and lead to different distributions.

This also holds in the above model if we keep only one pole, since the model is then equivalent to a real one by a shift $y \to y + \mu$.

Since the process automatically realizes a positive probability distribution $P(x, y)$ the change of sign in ρ cannot be taken care of by P itself but has to be reproduced by sign changes in the observables.

Pragmatic perspective: try to $ad\ hoc$ repair the procees, aiming at understanding its features (looking at the response).

For the real case with sign problem we use the above model with one pole and $\beta = 0$, $\mu = 0$. The above observations can be checked making ρ positive by:

Additive reweighting.

For any observable satifying $\int \mathcal{O} = 0$ (e.g., e^{inx}) we can rewrite $\langle \mathcal{O} \rangle$ as

$$\langle \mathcal{O} \rangle_\rho = \frac{\langle \mathcal{O} \rangle_\sigma}{\langle \rho/\sigma \rangle_\sigma} , \quad \sigma = \rho + c \tag{45}$$

with $c = constant$, since we have

$$\langle \mathcal{O} \rangle_\rho = \frac{\int \rho \mathcal{O}}{\int \rho} = \frac{\int \sigma \mathcal{O}}{\int \rho} = \frac{\int \sigma \mathcal{O}}{\int \sigma} \frac{\int \sigma}{\int \rho} . \tag{46}$$

We thus run CLE with real drift derived from the positive density σ and correct the normalization as shown above.

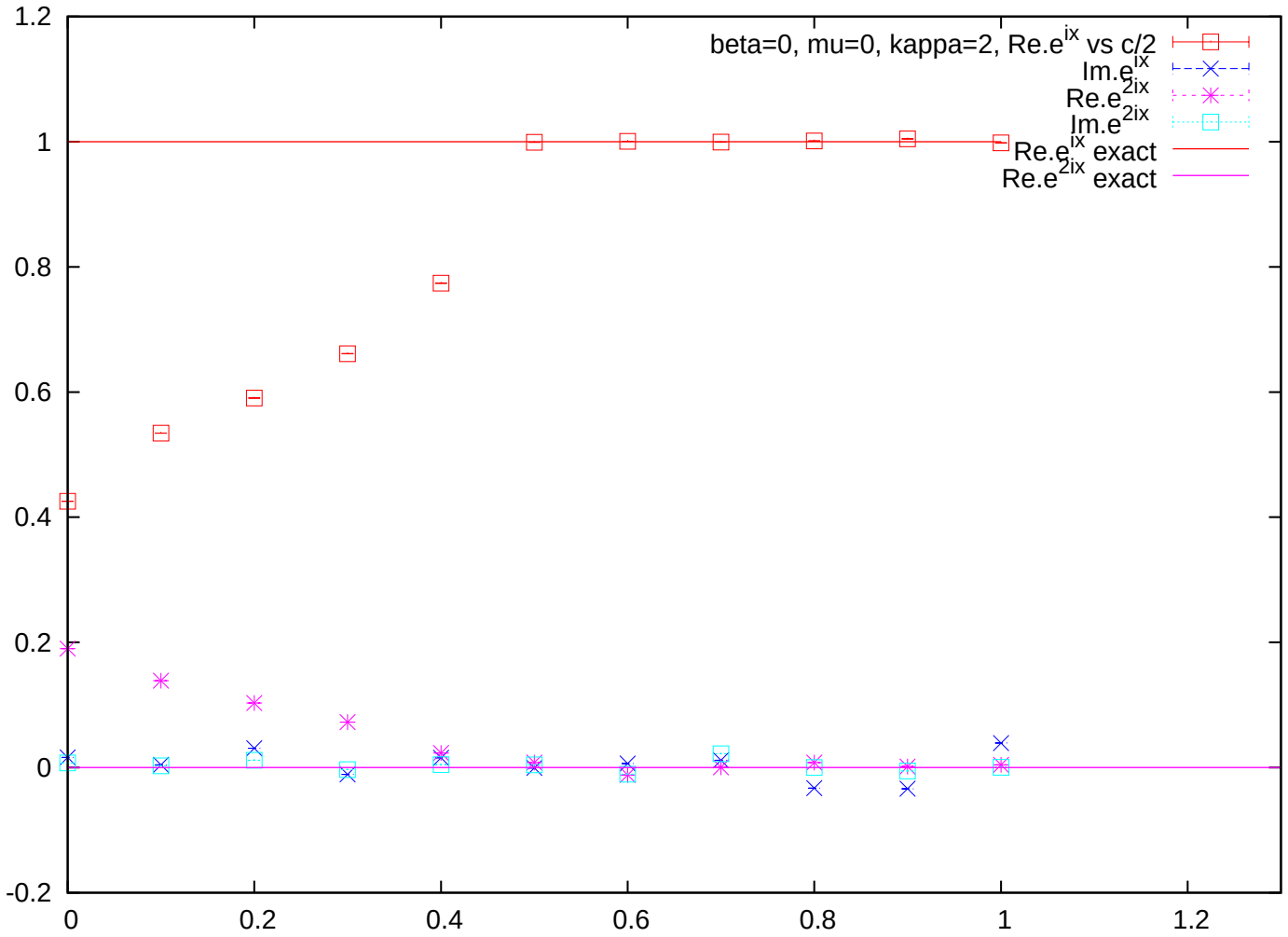

Figure 14: Real model for $\kappa = 2, \mu = \beta = 0$; data points: CLE with additive reweighting vs $c/2$, random complex starting points; solid lines: exact results.

In the complex case the situation is similar. For "small" β, $\kappa > 1$ we observe wrong convergence.

Observation: apparently the process does not sample correctly the regions of negative determinant. We check this observation using

Sign reweighting:

correct for the sign of the determinant in the observables:

$$\langle O(z)\rangle_{corr} = \frac{\langle O(z)c(z)\rangle}{\langle c(z)\rangle}, \quad c(z) = \mathrm{sgn} Re \det(z) \tag{47}$$

Notice: this is not the usual reweighting, the process is still complex!

For more then one pole we have an irreducible complex model. We can apply sign correction in the same way as for one pole.

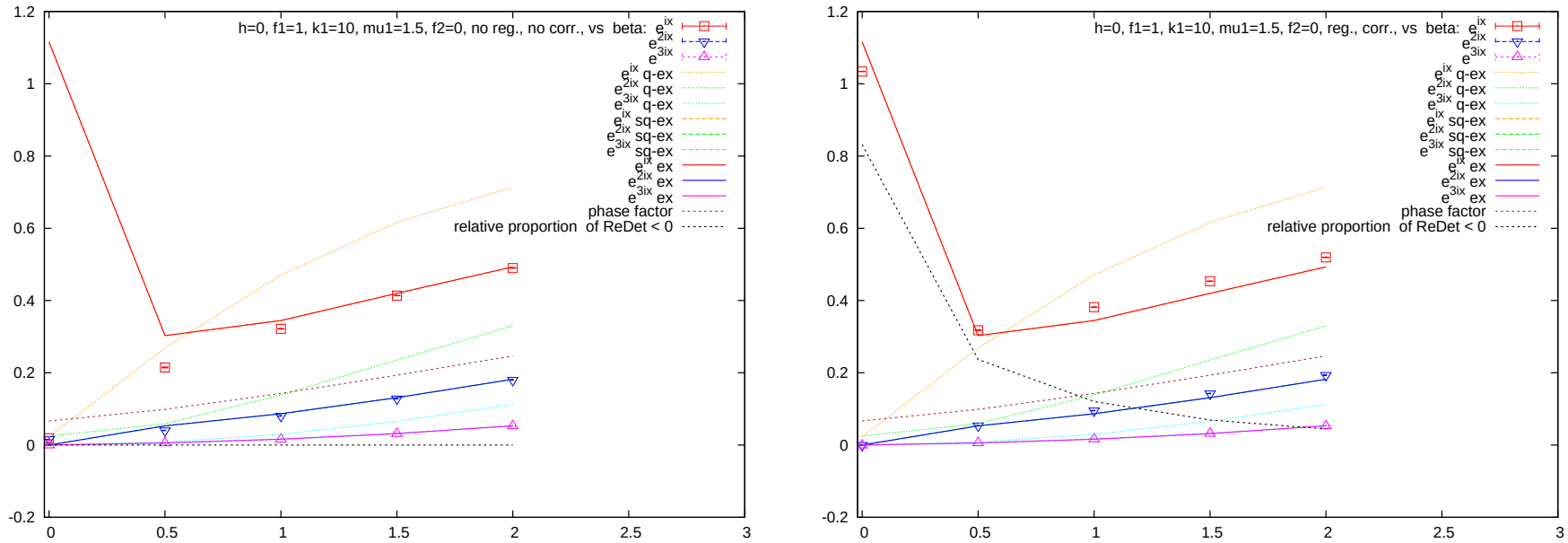

Figure 15: **Effect of one pole**, large κ vs β, uncorrected (left) and with an sign reweighting (right)

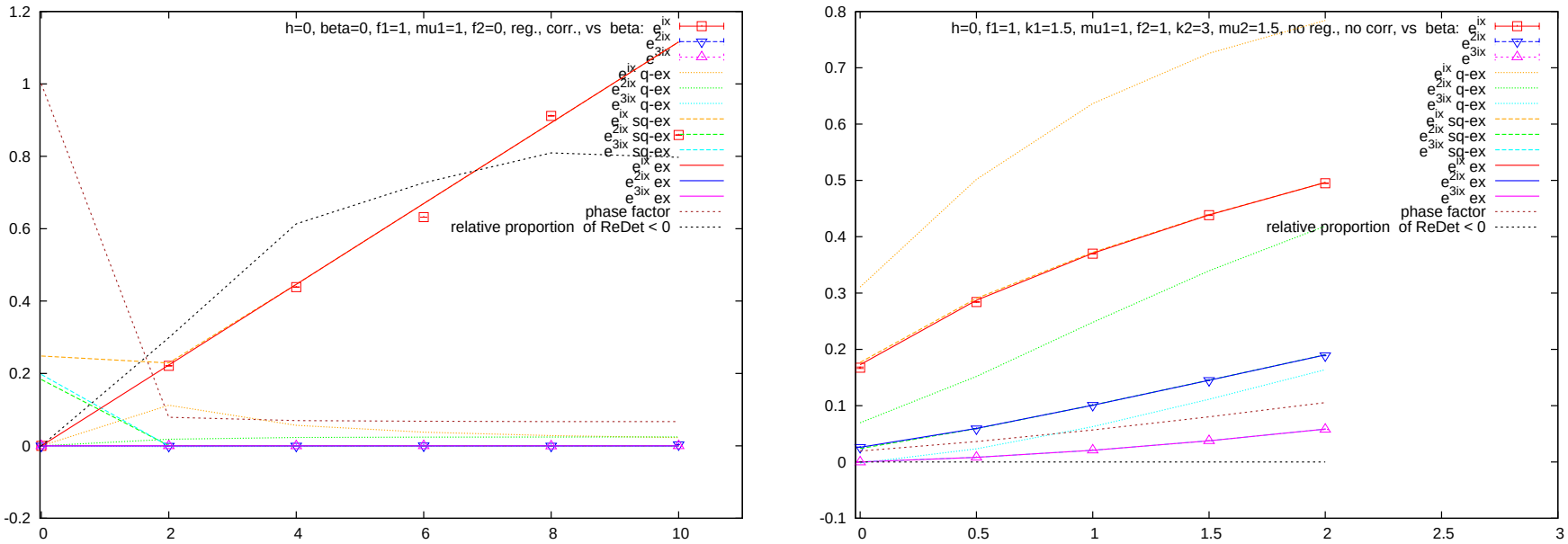

Figure 16: **Effect of one pole**, $\beta = 0$ vs κ with (left) and of two poles $\kappa > 1$ vs β without sign reweighting (right).

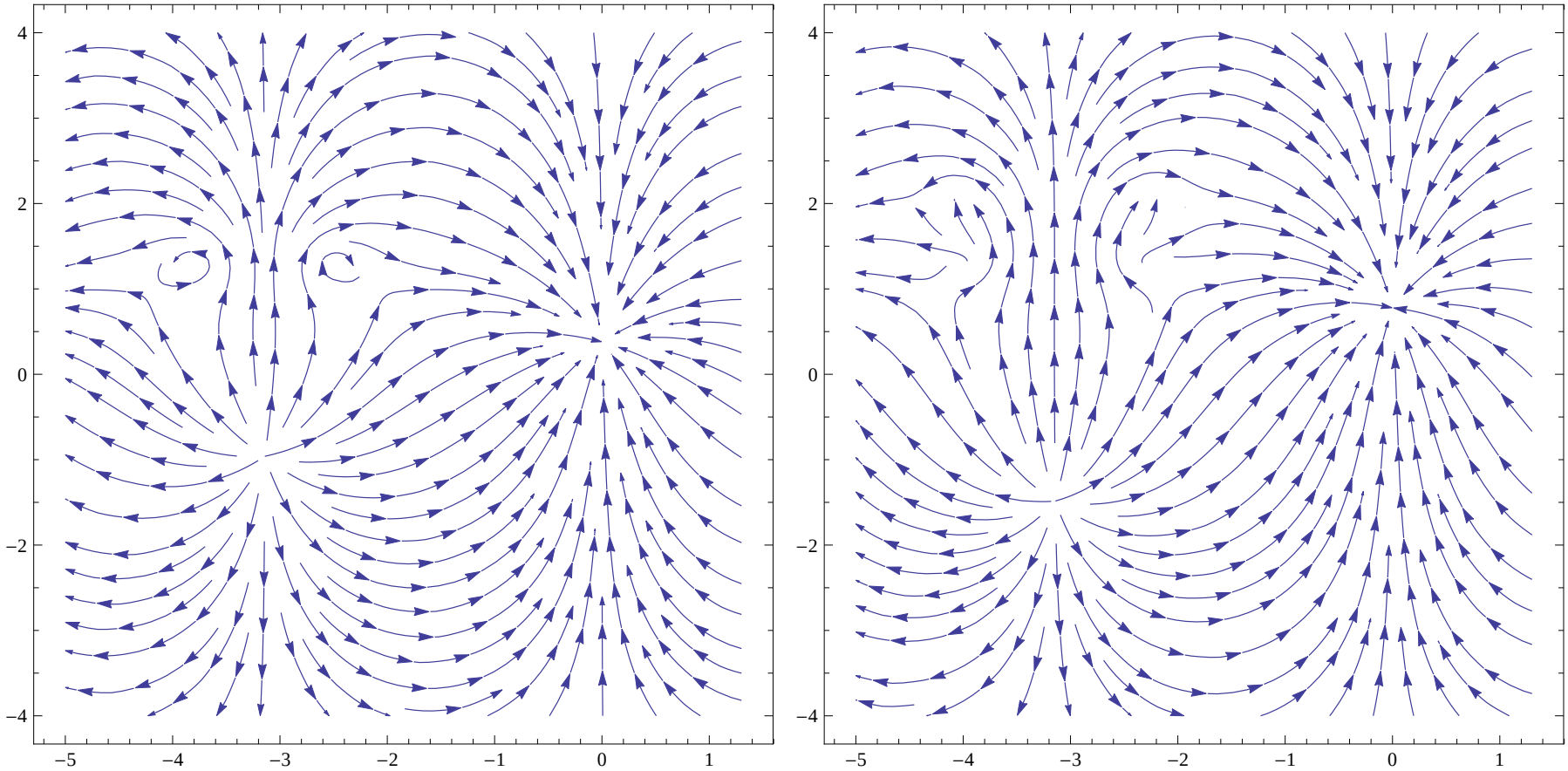

Figure 17: Flow diagram for one pole, $\beta = 1, \kappa = 2, \mu = 1$ (left) and for two poles (additional at $\kappa = 3, \mu = 2$) (right).

For more complex models the response to such redefinitions may differ (cf. *K. Splittorff, private communication*), which may mean that there are also other effects at work.

We learn from these exercises that:

- under certain conditions zeroes of ρ may lead to sign problems.
- these problems may be countered by forcing the process to sample regions where the change of sign is taken over by the observables.
- reweighting procedures of the above kind combined with CLE may work but our ambition is to reconstruct the CLE itself.

8.4 Effective model

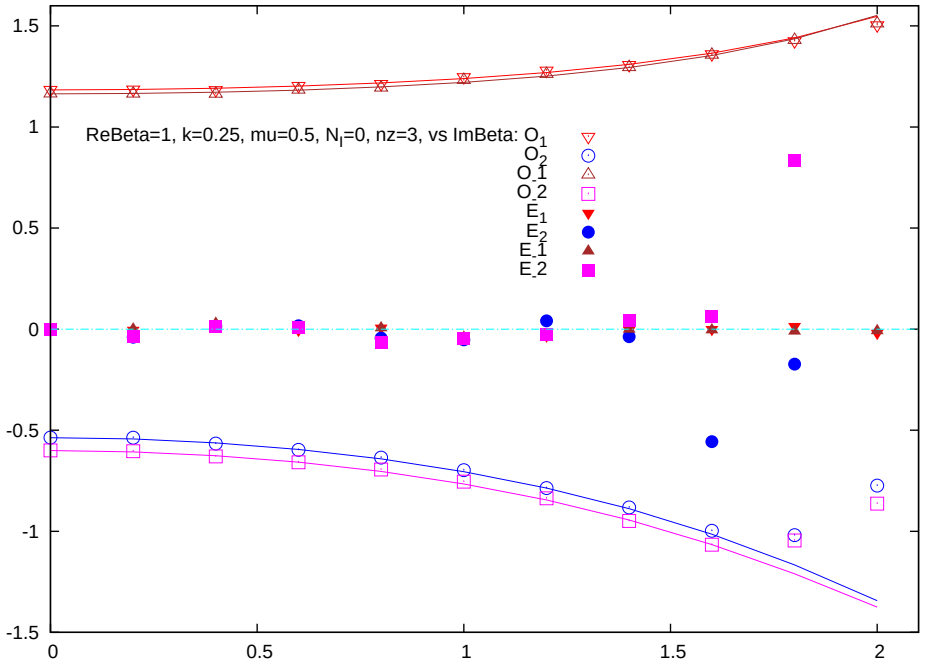

Figure 18: Effective model: Observables and CC's vs $Im\beta$, for $\alpha_i = 1$. The violation of the CC's signalizes discrepant results.

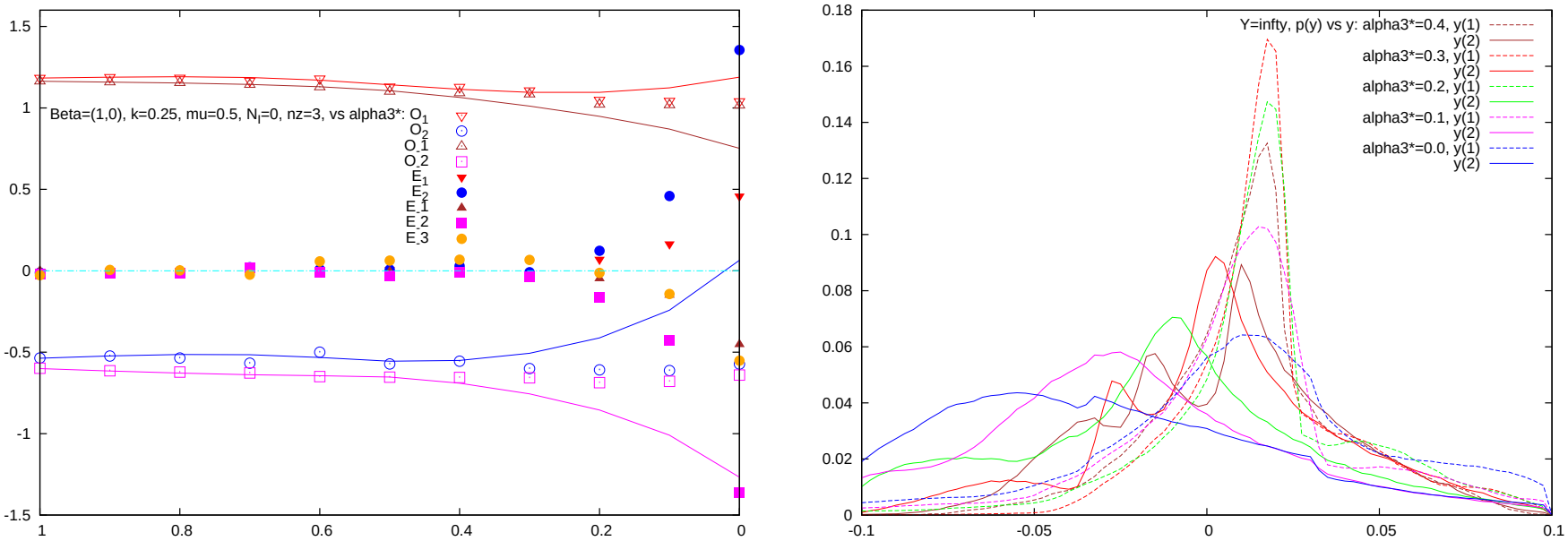

Figure 19: Effective model: Observables and CC's vs α_3 (left) and correspondig distributions (right).

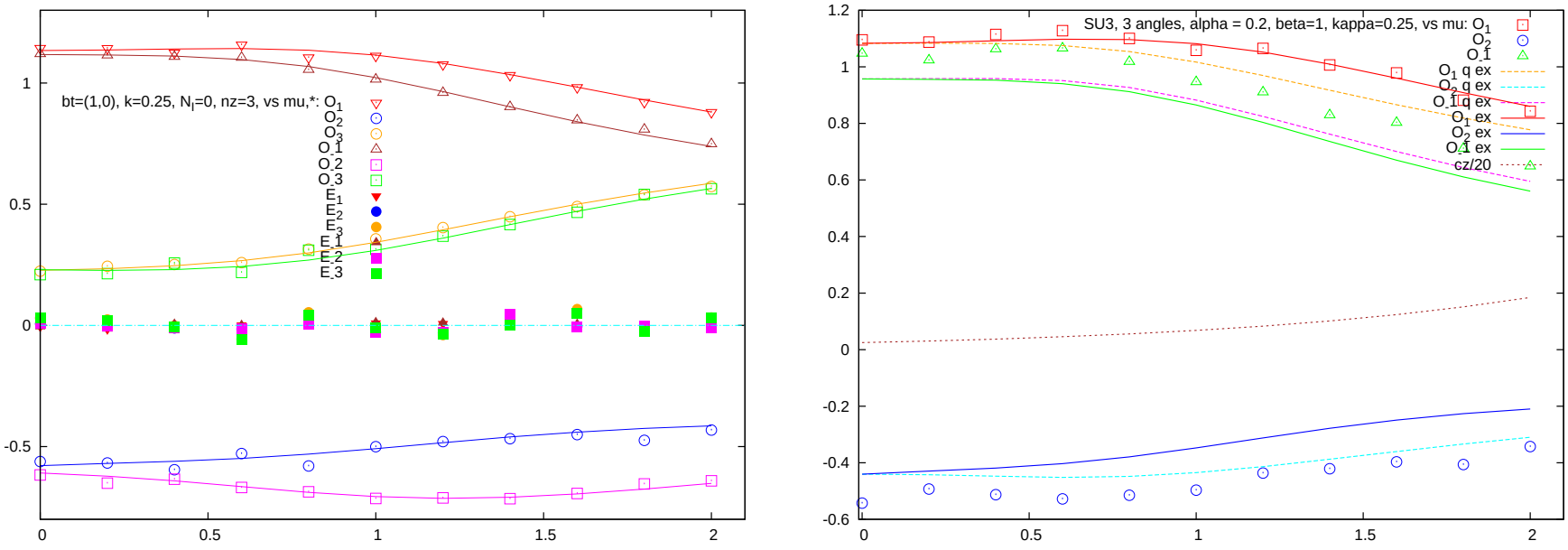

Figure 20: Effective model, μ dependence in the "good" (left) and in the "bad" region (right).

8.5 Hopping parameter expansion, systematic approximation

IOS (1982), Smit, Kawamoto (1982):

$$\begin{aligned} \mathrm{Det}\, W &= \exp(\mathsf{Tr} \ln W) \\ &= \exp\left[-\sum_{l=1}^{\infty} \sum_{\{\mathcal{C}_l\}} \sum_{s=1}^{\infty} \frac{\left(\kappa_\lambda^l g_{\mathcal{C}_l}\right)^s}{s} \mathsf{Tr}_{\mathrm{D,C}} \mathcal{L}_{\mathcal{C}_l}^s \right] \\ &= \prod_{l=1}^{\infty} \prod_{\{\mathcal{C}_l\}} \mathrm{Det}_{\,\mathrm{D,C}} \left(1 \; - \; (\kappa_\lambda)^l g_{\mathcal{C}_l} \mathcal{L}_{\mathcal{C}_l}\right) \end{aligned} \tag{48}$$

with $\mathcal{C}_l$ a closed, non-self-repeating path, λ the links on $\mathcal{C}_l$ and

$$\mathcal{L}_{\mathcal{C}_l} = \left(\prod_{\lambda \in \mathcal{C}_l} \Gamma_\lambda U_\lambda \right)^s \;, \; g_{\mathcal{C}_l} = \left(\epsilon \, \mathrm{e}^{\pm N_\tau \mu_f}\right)^r \; \text{or } 1 \tag{49}$$

with non-trivial $g_{\mathcal{C}_l}$ for loops winding r times in the ± 4 direction with periodic(antiperiodic) b.c. ($\epsilon = +1(-1)$) and $\kappa_\lambda = \kappa$ or $\kappa\,\gamma$ for spatial/temporal links.

8.6 Random Walk for CLE

A corresponding pair of real RW processes

$$\delta x(t) = \pm\omega_x\,, \quad P_{x,\pm} = \tfrac{1}{2}\left(1 \pm \frac{\omega_x}{2} Re\, K(z,t)\right) \tag{50}$$

$$\delta y(t) = \pm\omega_y\,, \quad P_{y,\pm} = \tfrac{1}{2}\left(1 \pm \frac{\omega_y}{2} Im\, K(z,t)\right) \tag{51}$$

$$\omega_x = \sqrt{2N_R\delta t}\,, \; \omega_y = \sqrt{2N_I\delta t} \tag{52}$$

where $P_\pm$ are *real* transition probabilities and we have defined the steps such as to have the same δt in all processes, to ensure the correct synchonization between them.

8.7 Staggered determinant in full QCD

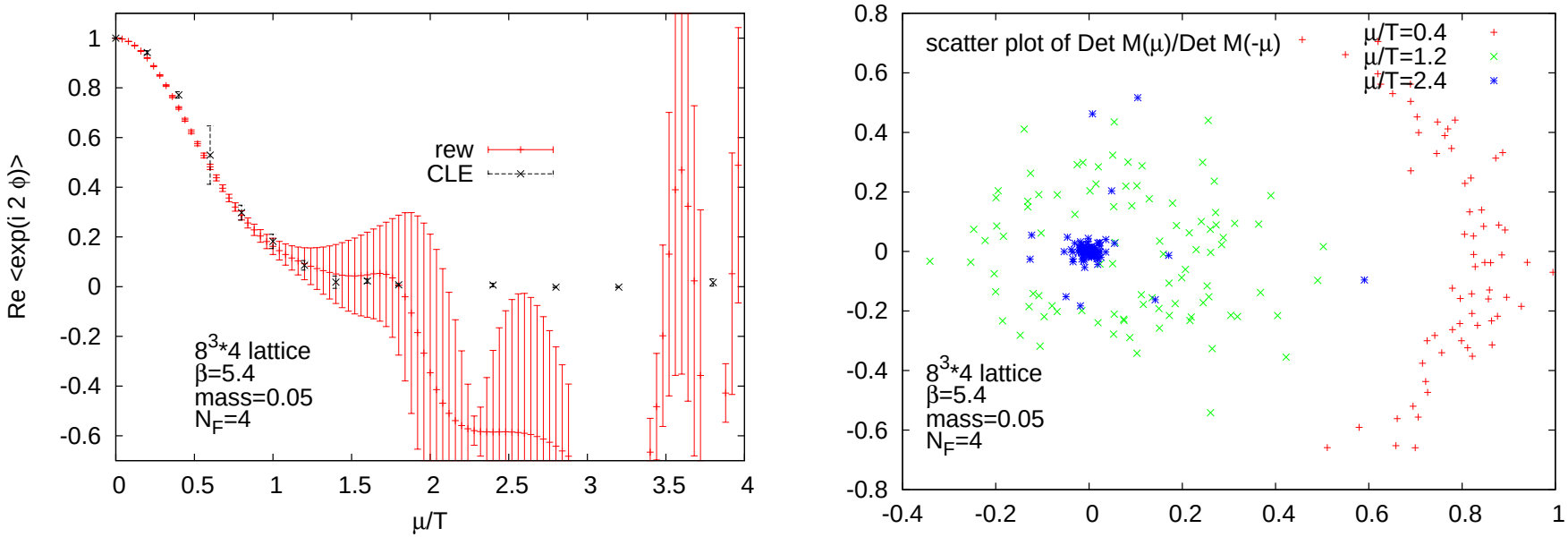

Figure 21: Phase average $\langle \det(\mu)/\det(-\mu) \rangle$ (left) and scatter plots of the phase (right), QCD with staggered fermions.

8.8 More figures ...

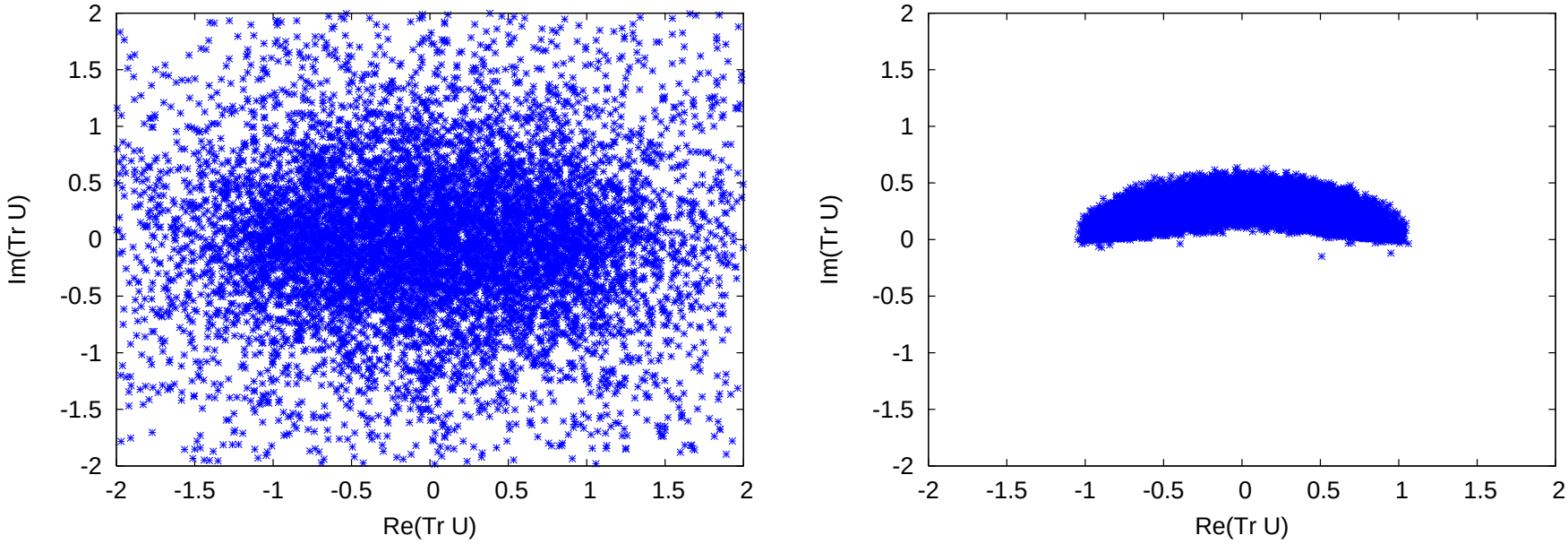

Figure 22: SU(2) one-link model: scatter plots of $\mathrm{Tr}\, U$ without and with gauge fixing, at $\beta = i$.

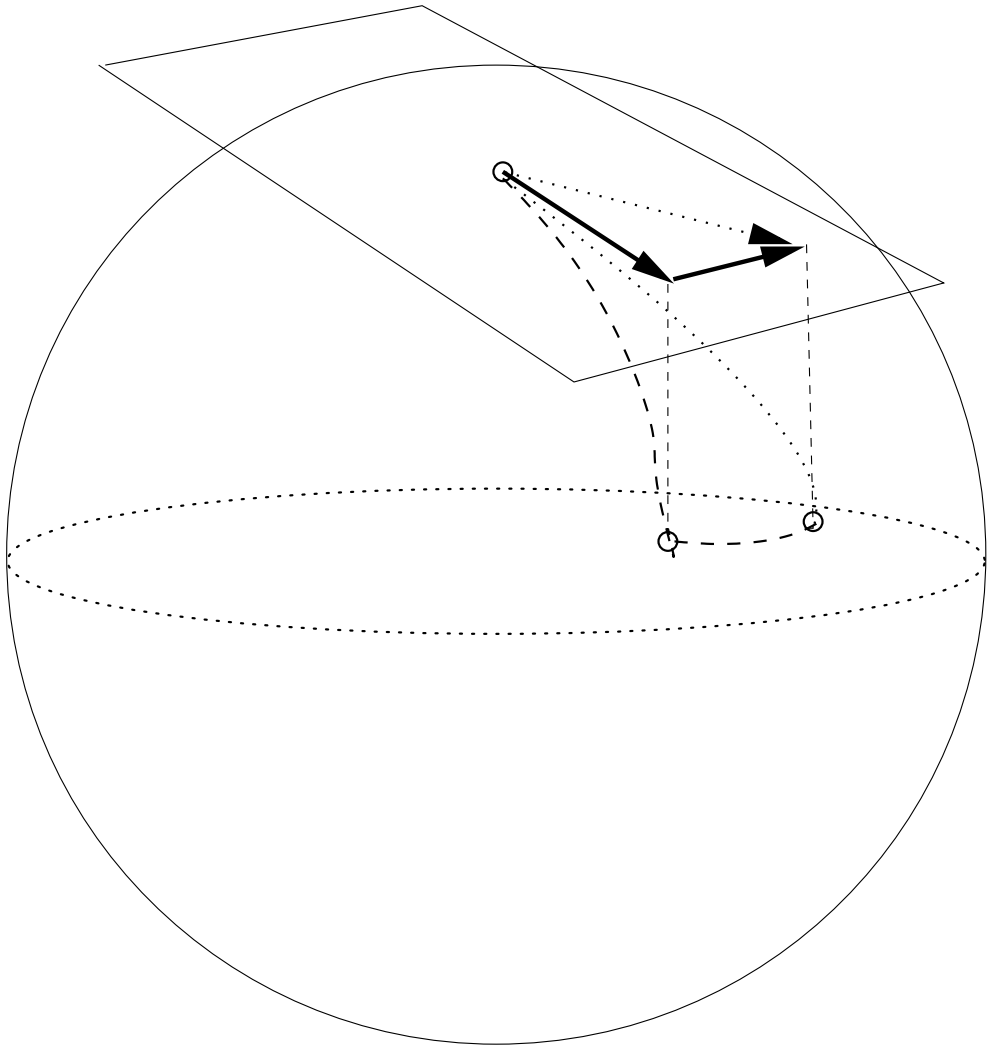

Figure 23: $SU(3)$ updating.

Little cooling, "numerical" exponentiation.

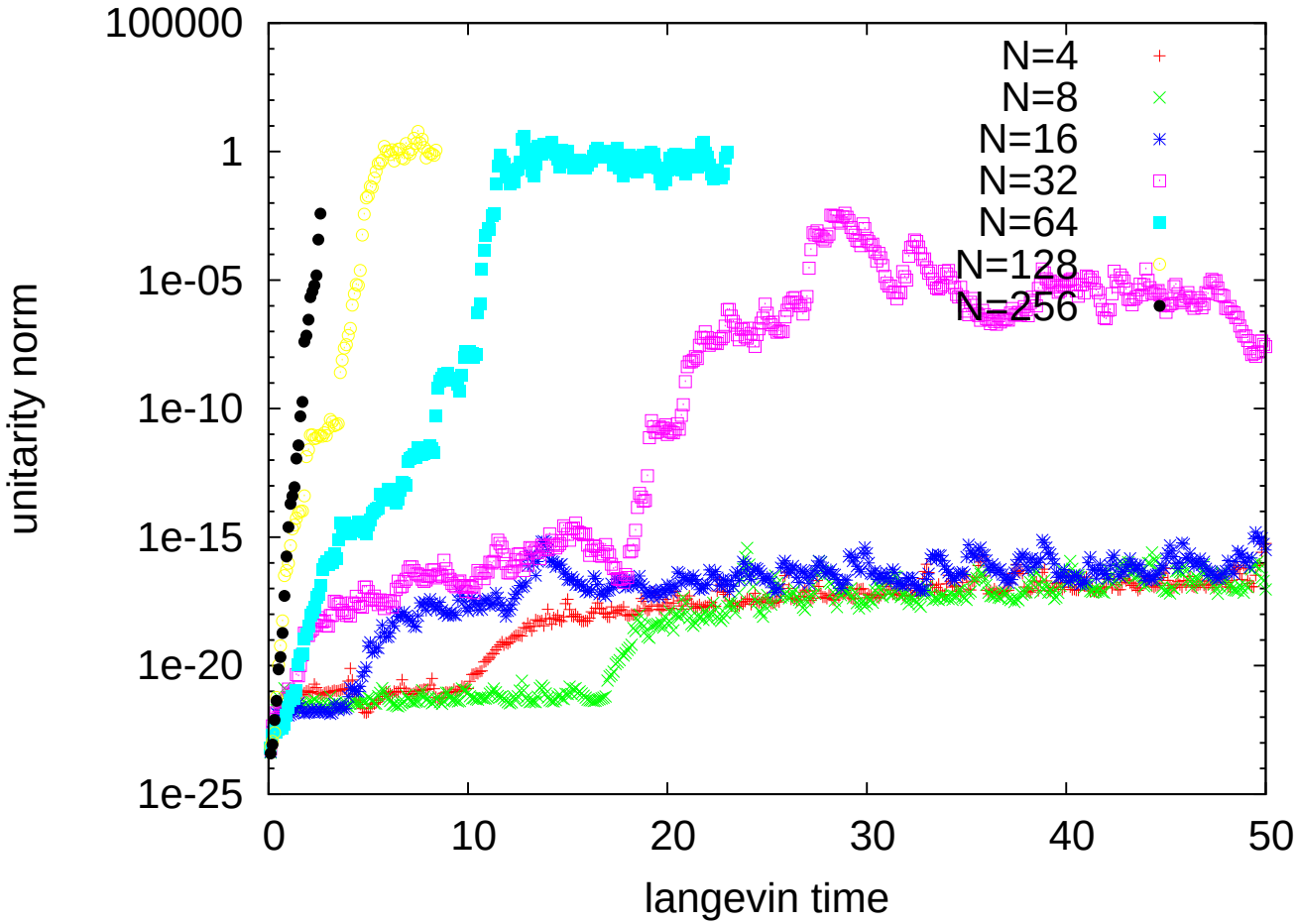

Figure 24: Polyakov chain, euclidean case ($\mu = 0$): evolution of the *UN* in langevin time t for various n; $\alpha = 0.0001$.

Dependence on cooling, "numerical" exponentiation.

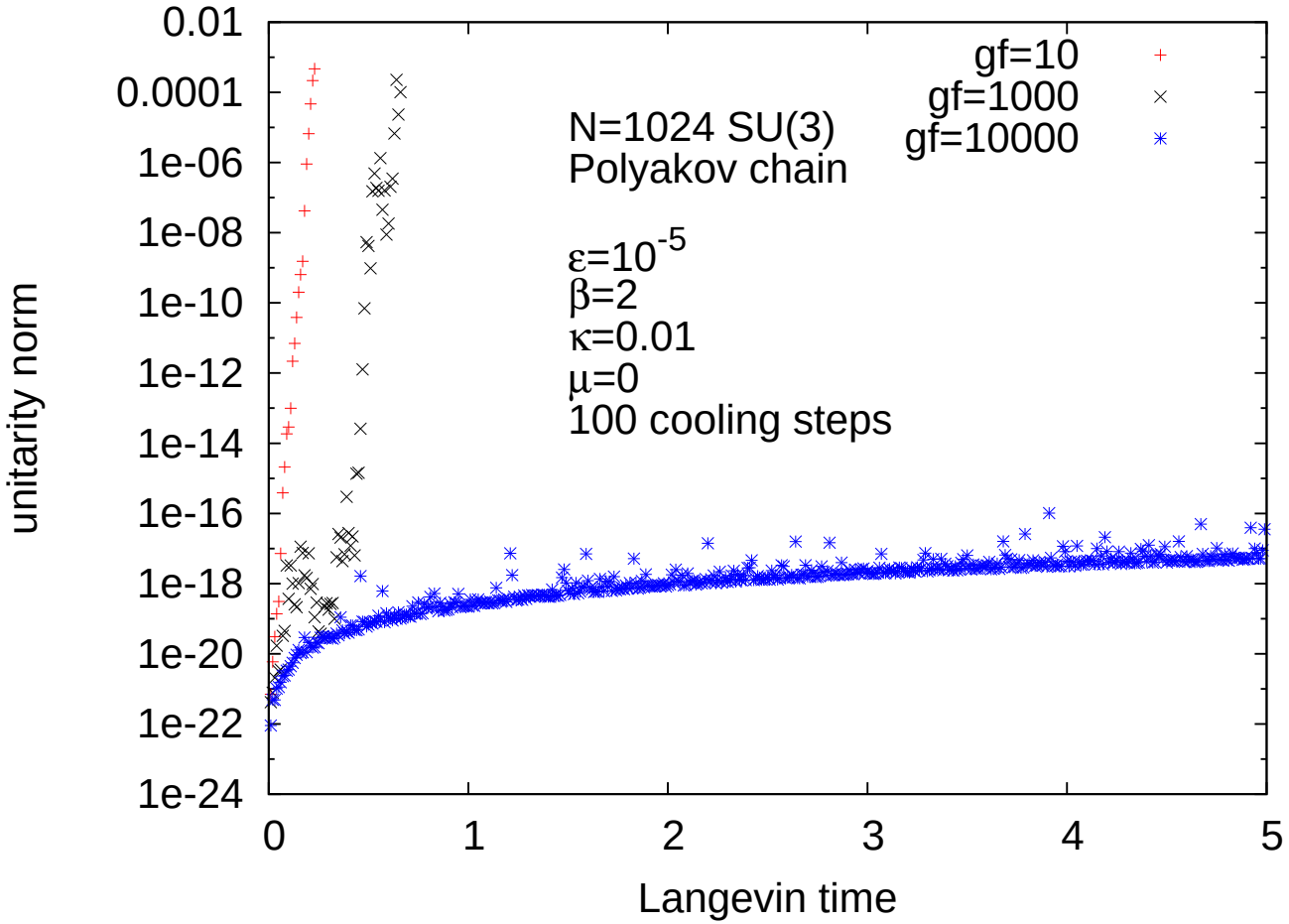

Figure 25: Polyakov chain, euclidean case: evolution of the *UN* in langevin time t for various $\alpha(= gf)$.

General (complex) case, “numerical” exponentiation.

Dependence on step size ϵ.

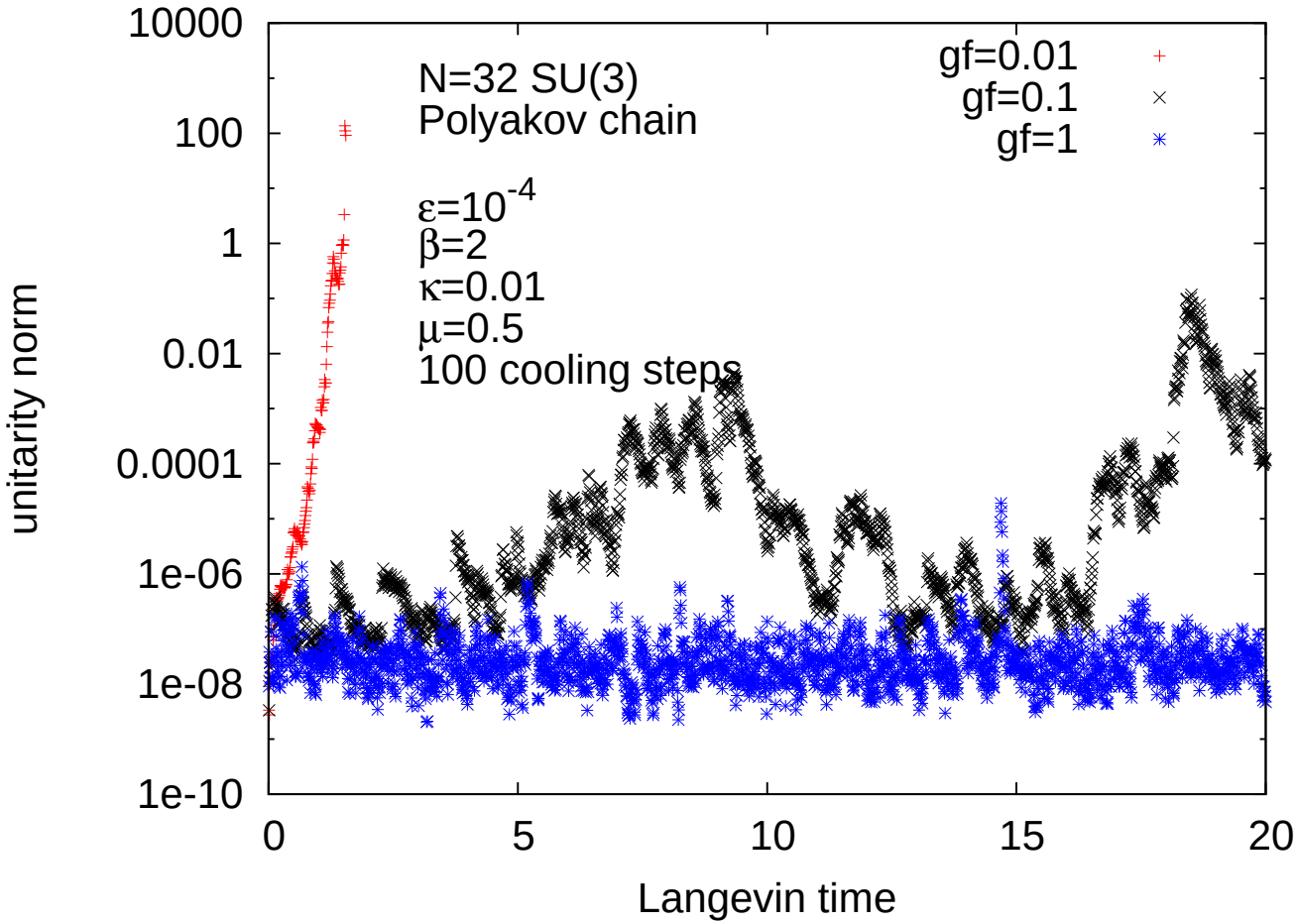

Figure 26: Polyakov chain, complex case: evolution of the *UN* in langevin time t for various α.

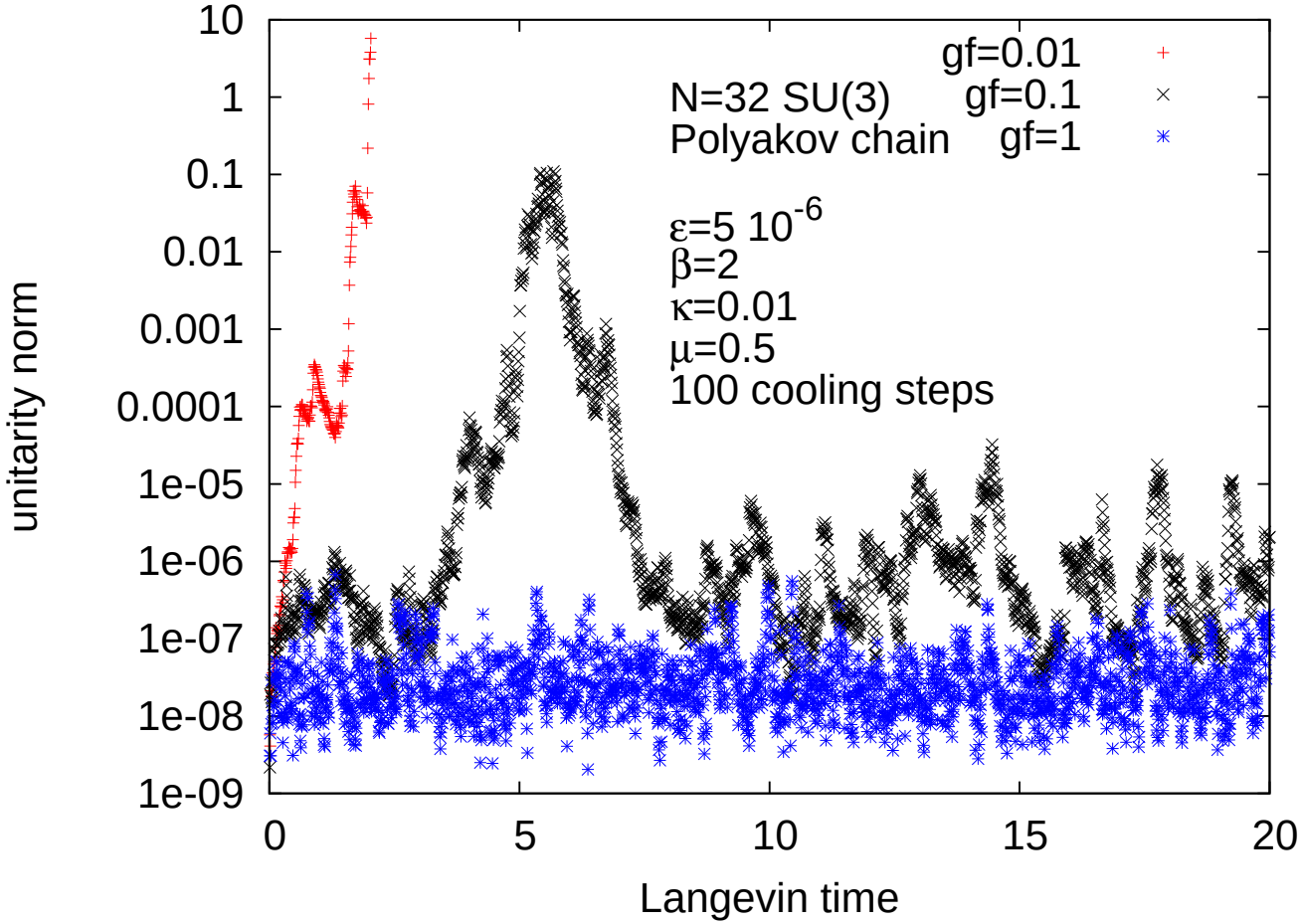

Figure 27: Polyakov chain, complex case: evolution of the *UN* in langevin time t for various α.

Dependence on cooling of the distribution ("numerical exponentiation").

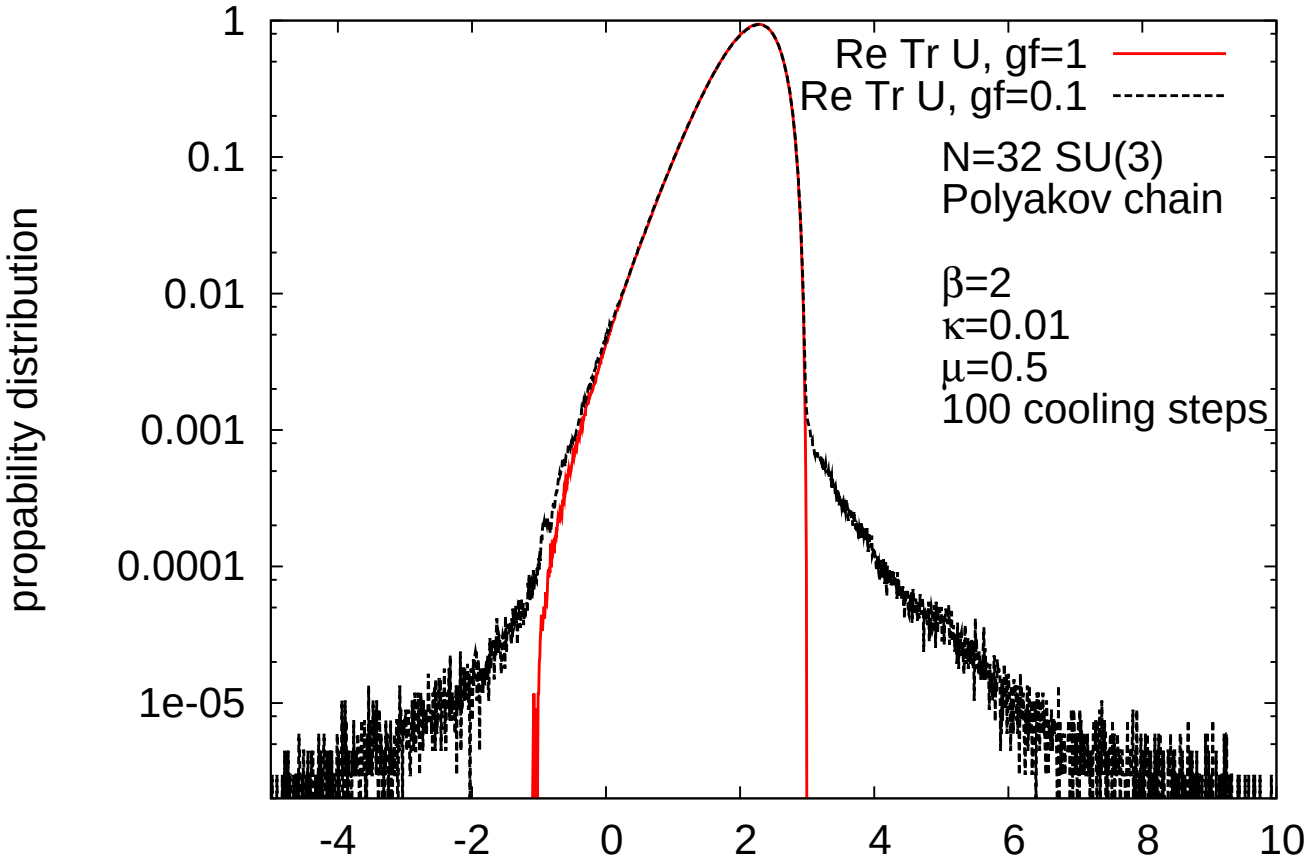

Figure 28: Distribution of the variables.

Dependence on α ("numerical exponentiation")

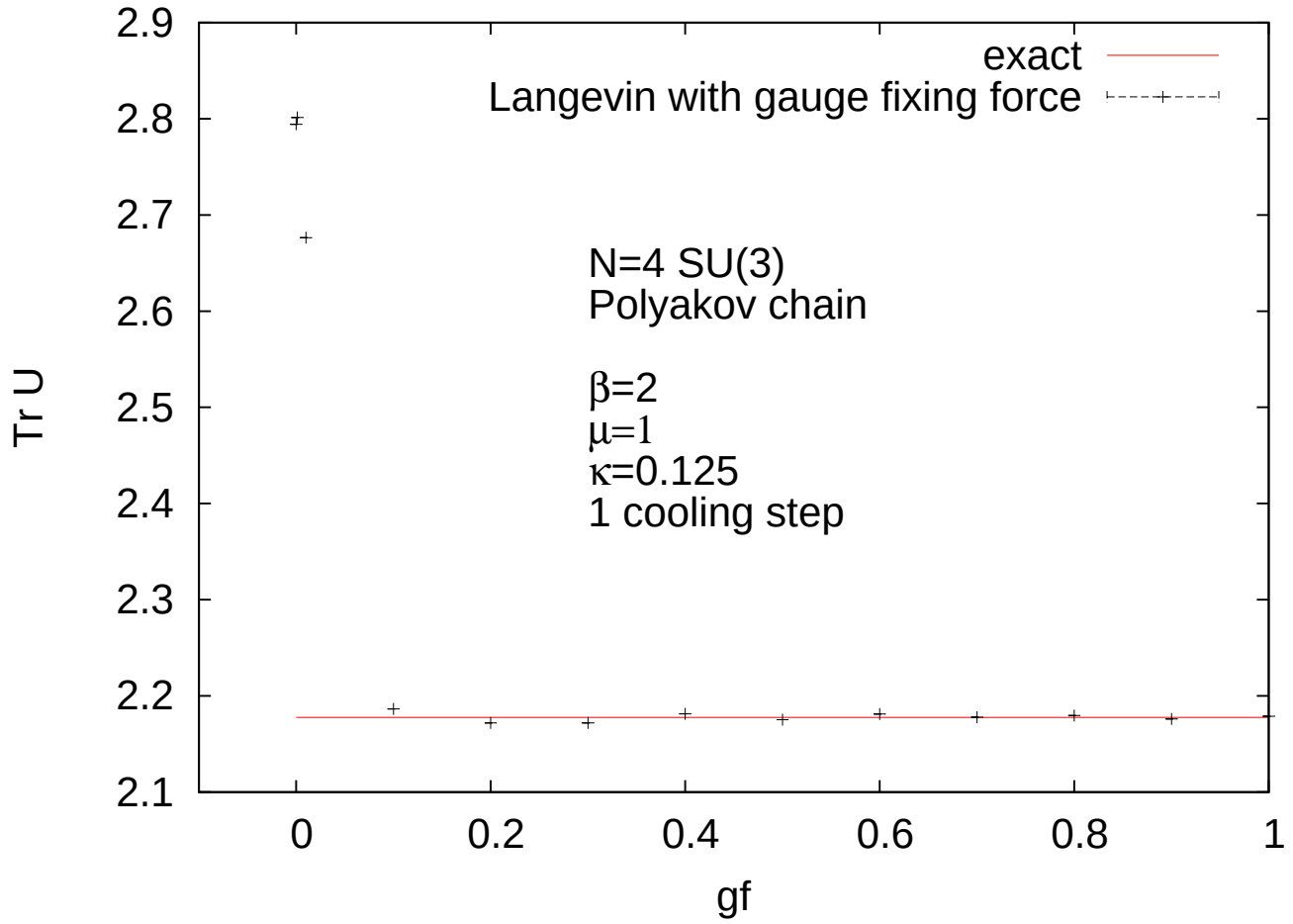

Figure 29: n=4 links.

Dependence on n ("analytic exponentiation"). The higher n the more cooling is necessary.

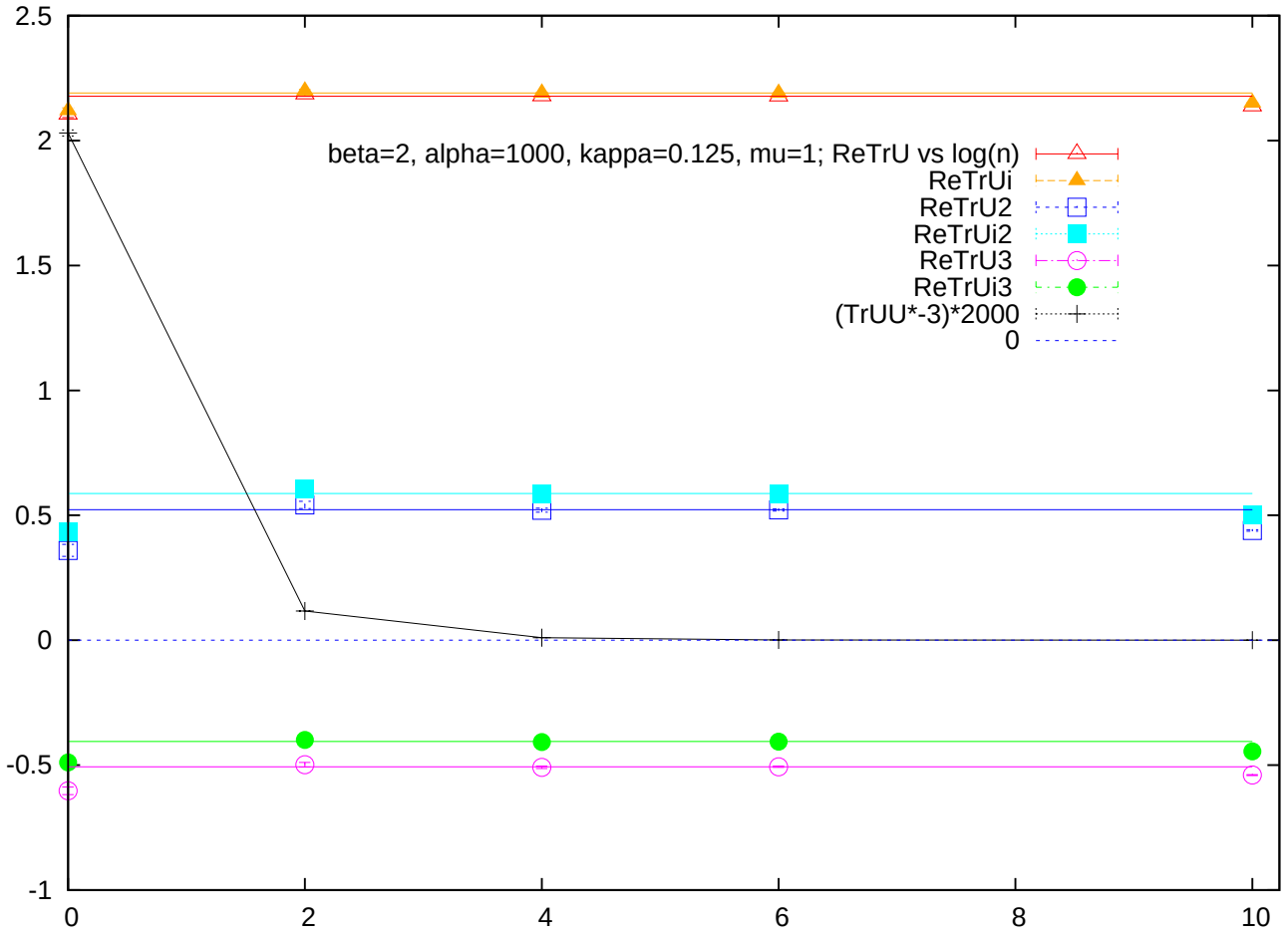

Figure 30: Observables vs $log_2(n)$. $1 \leq N \leq 100$, $1 \leq \alpha \leq 20000$.

Behaviour of the observables and of the unitarity norm. ("analytic exponentiation")

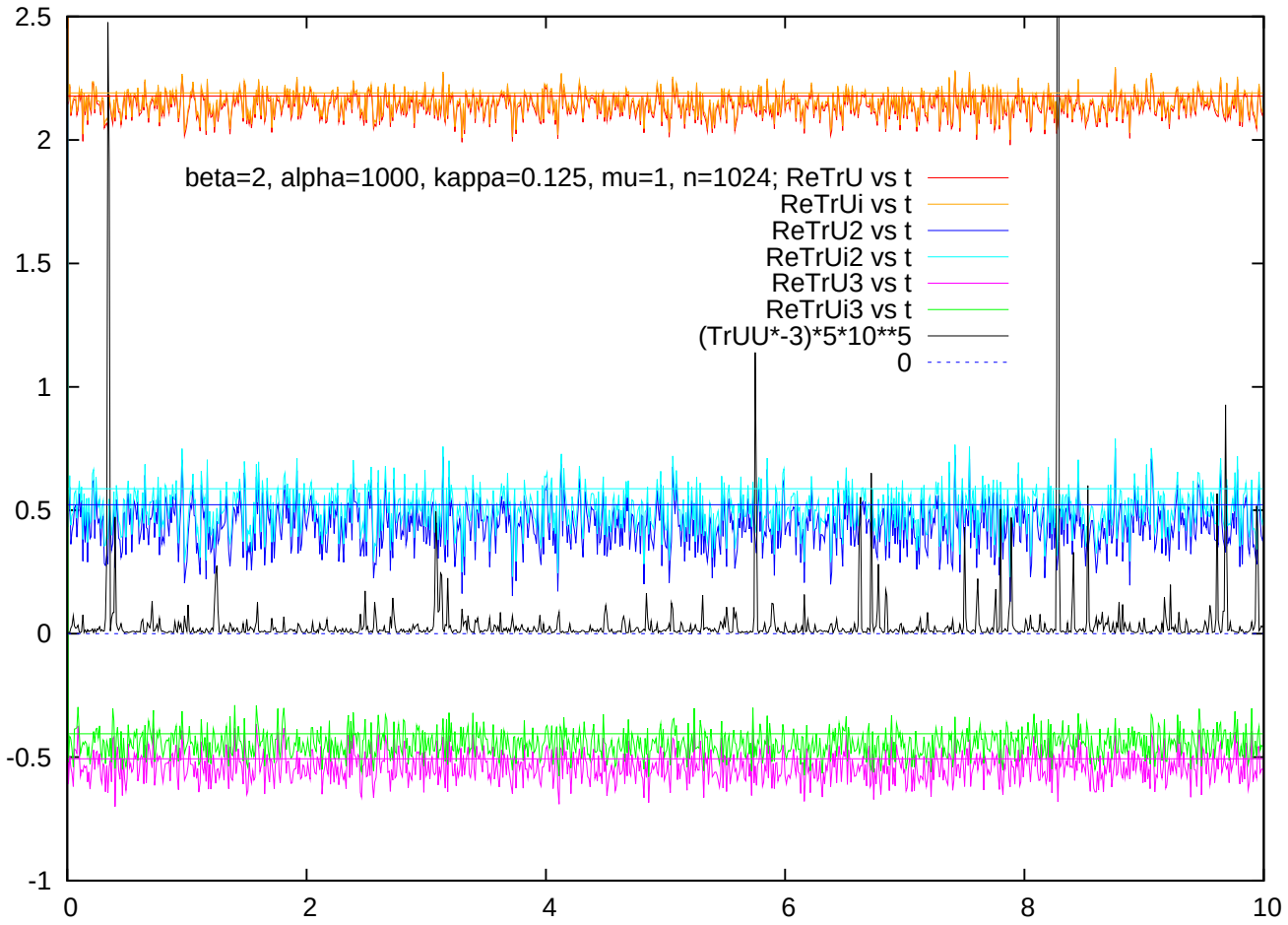

Figure 31: Evolution in langevin time t for $n = 1024$, $\alpha = 20000$, 50 cooling sweeps after each dynamical sweep.

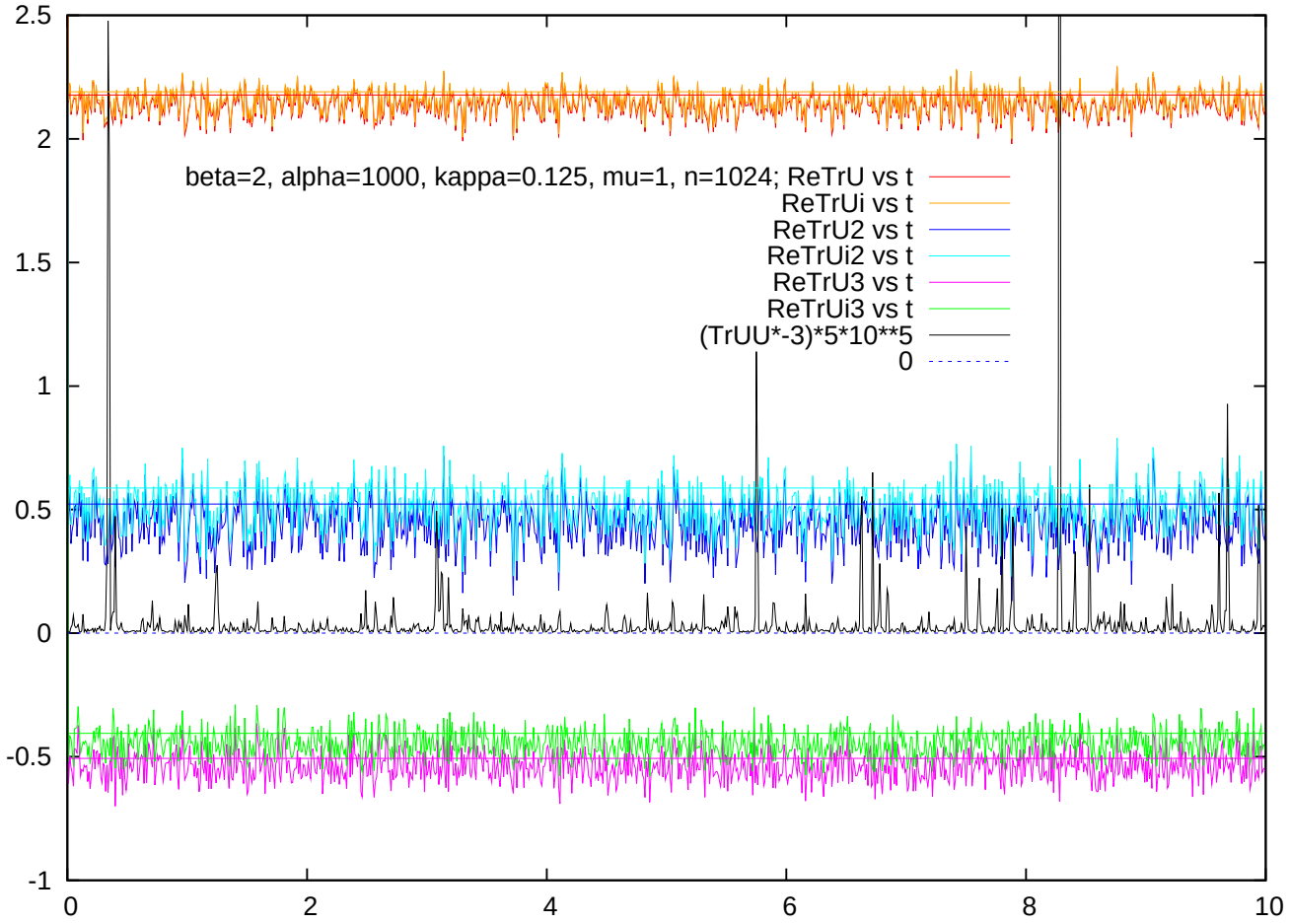

Figure 32: Evolution in langevin time t for $n = 32$, $\alpha = 20000$, $N = 50$ cooling sweeps after each dynamical sweep.

Lattice QCD with chemical potential, HDM approximation

HDM-limit (0-th order):

$$\kappa \to 0,\ \mu \to \infty,\quad \zeta = \kappa\, \mathrm{e}^{\mu}\ : fixed \tag{53}$$

only the Polyakov loops survive.

Higher order corrections: κ^2 , κ^4 are straightforward (combinatorics).

The determinant factorizes.